Towards Pre-trained Graph Condensation via Optimal Transport

Yeyu Yan[1,2], **Shuai Zheng**[1,2], **Wenjun Hui**[1,2], **Xiangkai Zhu**[3], **Dong Chen**[1,2], **Zhenfeng Zhu**[1,2*], **Yao Zhao**[1,2], **Kunlun He**[4]
[1]Institute of Information Science, Beijing Jiaotong University, China
[2]Visual Intelligence + X International Cooperation Joint Laboratory of the Ministry of Education, China
[3]Jinan University, China [4]Chinese PLA General Hospital, China
yanyeyu-work@foxmail.com, zs1997@bjtu.edu.cn,
22110090@bjtu.edu.cn, 18063597830@163.com, dchen2001@bjtu.edu.cn,
zhfzhu@bjtu.edu.cn, yzhao@bjtu.edu.cn, kunlunhe@plagh.org

Abstract

Graph condensation (GC) aims to distill the original graph into a small-scale graph, mitigating redundancy and accelerating GNN training. However, conventional GC approaches heavily rely on rigid GNNs and task-specific supervision. Such a dependency severely restricts their reusability and generalization across various tasks and architectures. In this work, we revisit the goal of ideal GC from the perspective of GNN optimization consistency, and then a generalized GC optimization objective is derived, by which those traditional GC methods can be viewed nicely as special cases of this optimization paradigm. Based on this, **Pre**-trained **G**raph **C**ondensation (**PreGC**) via optimal transport is proposed to transcend the limitations of task- and architecture-dependent GC methods. Specifically, a hybrid-interval graph diffusion augmentation is presented to suppress the weak generalization ability of the condensed graph on particular architectures by enhancing the uncertainty of node states. Meanwhile, the matching between optimal graph transport plan and representation transport plan is tactfully established to maintain semantic consistencies across source graph and condensed graph spaces, thereby freeing graph condensation from task dependencies. To further facilitate the adaptation of condensed graphs to various downstream tasks, a traceable semantic harmonizer from source nodes to condensed nodes is proposed to bridge semantic associations through the optimized representation transport plan in pre-training. Extensive experiments verify the superiority and versatility of PreGC, demonstrating its task-independent nature and seamless compatibility with arbitrary GNNs.

1 Introduction

Graph neural networks (GNNs) have emerged as a powerful approach to graph data analysis, showing excellent efficacy in a variety of domains, such as recommender systems [5], text analysis [56, 53], social network analysis [52], and so on. However, the dual challenges of exponentially growing graph data volumes [58] and increasingly sophisticated GNN architectures [63] present significant obstacles for GNN training. These challenges become particularly acute in scenarios that require multiple GNN training, such as continual graph learning [21] and federated graph learning [30].

In response to the above issues, graph condensation (GC) [25, 64] is proposed to optimize and synthesize a small-scale condensed graph from the real graph. The core objective is to ensure that

*Corresponding author

39th Conference on Neural Information Processing Systems (NeurIPS 2025).

condensed graphs achieve comparable performance as original graphs when training the same GNN. This approach significantly reduces computational overhead and becomes an up-and-coming solution for efficient graph learning. Depending on matching strategies, GC fall mainly into three types. For example, [25, 24, 55] distilled the properties of the real graph by mimicking its gradient changes in GNN training. [64, 59] replicated the training trajectory on original graphs to synthesize condensed graphs. Other studies [32, 16] generated the graph by aligning the latent space representations of both graphs and maintaining the distribution consistency. Recently, [16] pointed out that all these methods can be generalized as distribution matching, with the basic pipeline shown in Fig. 1 (a).

Despite these significant efforts, current methods suffer from two critical limitations: **(i) Architecture-bound optimization.** Current methods can be regarded as condensing through constraints in the same representation space [16]. Therefore, they have to adopt a fixed encoder to map nodes from the graph space to the representation space in condensation. Such an excessive dependence on a specific architecture can degrade the generalization of condensed graphs, leading to poor performance on other models. In addition, the learnable model parameters inherit task bias [46], which causes another challenge. **(ii) Task-constrained condensation.** To simplify optimization [25], existing methods typically assume that tasks and labels are known, thus the effectiveness of GC depends heavily on the guidance of supervision signals. Unfortunately, this assumption often proves impractical in real-world scenarios. For example, in social networks, multiple tasks may coexist (e.g., preference classification, income prediction, and relation prediction) [12], and user labels frequently vary owing to privacy constraints and annotation discrepancies [30]. When the task or label changes, conventional GC methods require re-condensation to capture new knowledge, significantly diminishing the reusability of condensed graphs. Although [15] attempted to address label dependency by contrastive learning, its reliance on class similarity hinders its application to other supervised tasks.

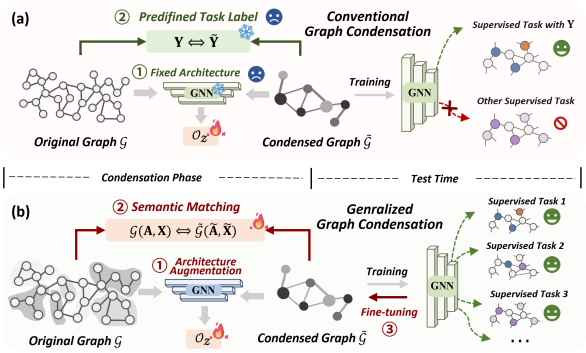

Figure 1: (a) The conventional GC framework. Due to specific ① architecture and ② task dependencies, $\tilde{\mathcal{G}}$ lacks generalization and reusability. (b) Our proposed generalized GC framework. It solves the above problems by ① and ②, and fine-tuning $\tilde{\mathcal{G}}$ in specific scenarios by ③.

To tackle the two critical challenges altogether, we first revisit the GC objective based on the goal of condensed graphs. It aims to achieve comparable performance to the original graph when training the same GNN (i.e. GNN optimization consistency). From this perspective, we derive a generalized GC optimization paradigm without task constraints as shown in Fig. 1 (b) and design a flexible and generalized GC method termed **Pre**-trained **G**raph **C**ondensation (PreGC). Inspired by data augmentation [10], graph diffusion augmentation is proposed to perturb node diffusion states via hybrid intervals, thereby enhancing the generalizability of condensed graphs and mitigating their dependence on specific architectures. To decouple the reliance on task labels, we present a novel matching mechanism, named transport plan matching. It maintains consistency in semantic associations between graph space and representation space, thus guaranteeing a unique mapping from each source node to its condensed counterpart. More importantly, transport plans provide explicit feedback on the significance of the source node, alleviating the poor traceability and interpretability issues in conventional condensation methods. After pre-training, a traceable semantic harmonizer via the optimal transport plan is derived, enabling flexible transfer of task signals from the original graph to the condensed graph for adaptation to diverse tasks.

To the best of our knowledge, PreGC is the first work for generalized graph condensation considering both architecture- and task-agnostic scenarios. Our main contributions are outlined as follows:

- Formal theoretical analysis reveals that conventional GC methods are inherently governed by the reconstruction term and the fitting term. Inspired by such an insight, we propose a pre-training framework of graph condensation, generalizing the condensed graph to more scenarios.

- To empower the condensed graph for architecture-agnostic scenarios, a hybrid-interval graph diffusion augmentation is presented, which enhances the diversity of node representations by introducing stochasticity into the diffusion process of both the condensed and original graphs.
- We propose an optimal transport plan matching to realize semantic alignment without task constrained. By keeping a consistent optimal plan for graph alignment and representation alignment, the uniqueness of semantic associations between source nodes and condensed nodes is guaranteed.
- Experiments on four mainstream tasks and nine representative GNN architectures demonstrate the superiority and generalization of PreGC. Further data valuation of the original graph highlights the PreGC's excellent traceability and interpretability.

2 Preliminary

Graph Condensation (GC). Given a large-scale original graph $\mathcal{G} = (\mathbf{A}, \mathbf{X})$ with a node set $\mathcal{V}$ ($|\mathcal{V}| = N$), where $\mathbf{A} \in \mathbb{R}^{N\times N}$ denotes the symmetrically normalized adjacency matrix and $\mathbf{X} \in \mathbb{R}^{N\times f}$ is a f-dimensional node feature matrix. GC [25, 33] aims to condense a small synthetic graph $\tilde{\mathcal{G}} = (\tilde{\mathbf{A}}, \tilde{\mathbf{X}})$ with a condensed node set $\tilde{\mathcal{V}}$ ($|\tilde{\mathcal{V}}| = M$) form the real large graph $\mathcal{G}$, where $\tilde{\mathbf{A}} \in \mathbb{R}^{M\times M}$, $\tilde{\mathbf{X}} \in \mathbb{R}^{M\times f}$, and $M \ll N$. At the same time, trained GNNs with the specific task have comparable performance on both $\tilde{\mathcal{G}}$ and $\mathcal{G}$, thus accelerating the training of GNNs.

Graph Optimal Transport. Optimal transport (OT) [39] aims to seek the most cost-efficient transport plan π that transforms a source distribution μ into a target distribution ν while minimizing the total transport cost (i.e., the optimal transport distance). The elements of π represent the probability of mass transferring from one location to another. In this work, we primarily concentrate on graph optimal transport [6, 43], which extends the OT to compare structured data. Given two graphs $\mathcal{G} = (\mathbf{A}, \mathbf{X})$ and $\tilde{\mathcal{G}} = (\tilde{\mathbf{A}}, \tilde{\mathbf{X}})$ with the nodes' empirical distribution $\mu \in \mathbb{R}^N$ and $\nu \in \mathbb{R}^M$, the general form of the graph optimal transport distance can be formalized as:

$$\mathcal{W}(\mathcal{G}, \tilde{\mathcal{G}}) = \min_{\pi\in\Pi(\mu,\nu)} \left\langle \mathcal{C}(\mathbf{X}, \tilde{\mathbf{X}}, \mathbf{A}, \tilde{\mathbf{A}}, \pi), \pi \right\rangle \tag{1}$$

where $\Pi(\mu, \nu) = \{\pi \in \mathbb{R}^{N\times M} | \pi\mathbf{1}_M = \mu, \mathbf{1}_N\pi = \nu\}$ is set of the joint distributions π with marginals μ and ν, and and $\langle\cdot,\cdot\rangle$ denotes the inner product for matrices. $\mathcal{C}$ represents the cost function that quantifies the cost of transporting mass from elements in one domain to another.

The transport distance quantifies the distribution divergence between condensed and original graphs, offering a novel optimization approach for GC. Meanwhile, the transport plan establishes explicit node correspondences, overcoming the limitations of poor traceability in conventional GC methods.

3 Revisiting and Generalizing Graph Condensation

In this section, we revisit the objective of graph condensation and reveal the limitations of existing GC methods, thus motivating the design of PreGC.

Revisiting. For convenience, we follow [33] and start with a vanilla example, which adopts a K-order SGC [48] as the GNN and simplifies the objective of GNNs into the MSE loss: $\mathcal{L}_{MSE} = \|\mathbf{A}^K\mathbf{X}\mathbf{W} - \mathbf{Y}\|_F^2$, where $\mathbf{Y} \in \mathbb{R}^{N\times C}$ denotes the target variable and $\mathbf{W} \in \mathbb{R}^{f\times C}$ is the model parameter. For the original graph $\mathcal{G}$, the optimal $\mathbf{W} = \arg\min_{\mathbf{W}} \|\mathbf{A}^K\mathbf{X}\mathbf{W} - \mathbf{Y}\|_F^2$ can be obtained by MSE loss. In general, the goal of condensation is that the GNN trained on the condensed graph $\tilde{\mathcal{G}}$ to achieve comparable performance to those trained on $\mathcal{G}$, i.e

$$\min \|\mathbf{W} - \tilde{\mathbf{W}}\|_F = \min \|(\mathbf{A}^K\mathbf{X})^\dagger\mathbf{Y} - (\tilde{\mathbf{A}}^K\tilde{\mathbf{X}})^\dagger\tilde{\mathbf{Y}}\|_F \tag{2}$$

where $\tilde{\mathbf{W}} = \arg\min_{\tilde{\mathbf{W}}} \|\tilde{\mathbf{A}}^K\tilde{\mathbf{X}}\tilde{\mathbf{W}} - \tilde{\mathbf{Y}}\|_F^2$ with target variable $\tilde{\mathbf{Y}} \in \mathbb{R}^{M\times C}$ on $\tilde{\mathcal{G}}$, and $\dagger$ denotes pseudo inverse. Subsequently, we further derive the following proposition (Proofs are in Appendix A):

Proposition 3.1. *Suppose that it has an analytical filter $g(\cdot)$ for a GNN model, the performance approximation error $\mathcal{O}_\mathcal{W}$ of condensed graph is jointly bounded by the reconstruction term $\mathcal{O}_\mathcal{Z}$ and the fitting term $\mathcal{O}_\mathcal{Y}$.*

$$\underbrace{\|\mathbf{W} - \tilde{\mathbf{W}}\|_F}_{\mathcal{O}_\mathcal{W}} \leq \|\boldsymbol{\mathcal{M}}_\mathcal{Z}(\mathbf{Y})\|_F \cdot \underbrace{\|\boldsymbol{\mathcal{M}}_\mathcal{Z}(g(\mathbf{L})\mathbf{X})^\dagger - (g(\tilde{\mathbf{L}})\tilde{\mathbf{X}})^\dagger\|_F}_{\mathcal{O}_\mathcal{Z}} + \underbrace{\|\boldsymbol{\mathcal{M}}_\mathcal{Z}(\mathbf{Y}) - \tilde{\mathbf{Y}}\|_F}_{\mathcal{O}_\mathcal{Y}} \cdot \|(g(\tilde{\mathbf{L}})\tilde{\mathbf{X}})^\dagger\|_F \tag{3}$$

where $\mathcal{M}_{\mathcal{Z}}(\cdot)$ is any mapping function that aligns $g(\tilde{\mathbf{L}})\tilde{\mathbf{X}}$ and $g(\mathbf{L})\mathbf{X}$ or $\tilde{\mathbf{Y}}$ and $\mathbf{Y}$. $\mathbf{L} = \mathbf{I}_N - \mathbf{A}$ and $\tilde{\mathbf{L}} = \mathbf{I}_M - \tilde{\mathbf{A}}$ are the Laplacian matrices of $\mathcal{G}$ and $\tilde{\mathcal{G}}$.

Proposition 3.1 reveals that the reconstruction term $\mathcal{O}_{\mathcal{Z}}$ and the fitting term $\mathcal{O}_{\mathcal{Y}}$ are the two key factors for ideal GC. Unfortunately, current GC methods rely on specific GNNs (i.e. the rigid filter $g(\cdot)$), resulting in spectrally limited condensed graphs with higher reconstruction errors for $\mathcal{O}_{\mathcal{Z}}$. Moreover, the pre-defined task signal in condensation restricts $\mathcal{O}_{\mathcal{Y}}$ to the specific task. Consequently, the condensed graph can only achieve satisfactory performance with the pre-defined GNNs and task, severely limiting its generalizability and reusability. To overcome these limitations, we focus on proposition 3.1 and relax the above conditionally constrained GC objective into a generalized one:

Definition 3.1. ***Generalized Graph Condensation.*** *Given an original graph $\mathcal{G}$, the objective of ideal graph condensation is to seek a condensed graph $\tilde{\mathcal{G}}$ that simultaneously minimizes the representation-level and the semantic-level discrepancies relative to $\mathcal{G}$:*

$$\tilde{\mathcal{G}}^* = \arg\min_{\tilde{\mathcal{G}}} \{ \underbrace{\Delta_{\mathcal{Z}}(\mathbf{Z}, \tilde{\mathbf{Z}})}_{\mathcal{O}_{\mathcal{Z}}} + \xi \underbrace{\Delta_{\mathcal{Y}}(\mathcal{G}, \tilde{\mathcal{G}})}_{\mathcal{O}_{\mathcal{Y}}} \} \tag{4}$$

where $\Delta_{\mathcal{Z}}(\cdot,\cdot)$ measures the representation-level discrepancy between representations $\mathbf{Z}$ and $\tilde{\mathbf{Z}}$ of $\mathcal{G}$ and $\tilde{\mathcal{G}}$. $\Delta_{\mathcal{Y}}(\cdot,\cdot)$ is a distance function measuring semantic-level discrepancy, and ξ serves as a trade-off parameter balancing the fitting and reconstruction terms.

Definition 3.1 presents a general GC optimization paradigm, of which current GC methods can be regarded as variant forms (Appendix C.2 shows more details). In this formulation, the generalized node representation $\mathbf{Z}$ replaces $g(\mathbf{L})\mathbf{X}$, and the task-specific fitting term $\mathcal{O}_{\mathcal{Y}}$ is relaxed to semantic alignment between two graphs. Therefore, by boosting the diversity of the representations $\mathbf{Z}$ and $\tilde{\mathbf{Z}}$, and designing unsupervised signals for $\Delta\mathcal{Y}$, it is possible to readily establish a pre-trained graph condensation framework. Such a framework enhances the generalization of the condensed graph and augments its adaptability across diverse scenarios.

4 Methodology

Fig. 2 illustrates the framework of PreGC, which strictly follows the GC objective in Eq. (4). In pre-training phase, graph diffusion augmentation is proposed to increase the diversity of representations in $\mathcal{O}_{\mathcal{Z}}$ to alleviate architectural dependencies. Subsequently, to realize task-agnostic graph condensation, PreGC adopts an innovative transport plan matching to align semantic associations in $\mathcal{O}_{\mathcal{Y}}$. In addition, test-time fine-tuning further achieves dynamic adaptation on specific tasks and architectures.

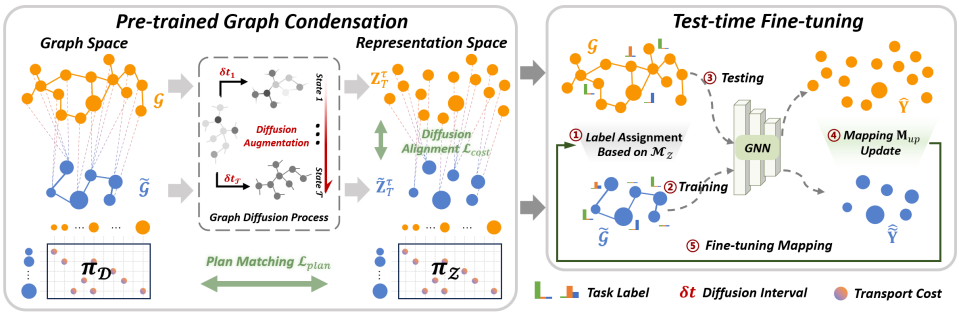

Figure 2: Overall pipeline of the proposed PreGC framework. $\pi_{\mathcal{D}}$ and $\pi_{\mathcal{Z}}$ denote optimal transport plans for graph alignment and for representation alignment, respectively.

4.1 Diffusion Augmentation via Graph Heat Equation

As analyzed in Section 3, most GC methods adopt K-order SGC [48] or GCN [26] for encoding graphs to obtain $\mathbf{Z}$ and $\tilde{\mathbf{Z}}$ [42]. However, parameters in neural networks may inherit task-induced biases, thus distorting the intrinsic representation properties. Although GDEM [33] and CGC [16] attempt to use parameter-free encoders to obtain node representations, they remain architecture-bound, resulting in condensed graphs hard to generalize to other GNNs. More critically, under discrete

propagation, the representation distributions of two graphs evolve at markedly divergent rates due to diameter disparities, inevitably exacerbating the difficulty of GC.

The graph heat equation (GHE) [9], as a generalization of the diffusion equation on graph data (graph diffusion), serves as an effective solution to the above problems due to its non-parametric and dynamic continuity properties. Formally, GHE can be defined as $\frac{d\mathbf{Z}_t}{dt} = -\mathbf{L}\mathbf{Z}_t$, where $\mathbf{Z}_t$ is the evolved input representation at time t, and $\mathbf{Z}_0 = \mathbf{X}$. In our proposed PreGC, graph diffusion [31] is used to encode node representations and solved using Explicit Euler method:

$$\mathbf{Z}_{t+\delta t} = \mathbf{Z}_t - \delta t\mathbf{L}\mathbf{Z}_t = \mathbf{A}^{(\delta t)}\mathbf{Z}_t \tag{5}$$

where δt is diffusion interval and $\mathbf{A}^{(\delta t)} = (1-\delta t)\mathbf{I} + \delta t\mathbf{A}$. Finally, the representation (or state) $\mathbf{Z}_T$ at the terminal time $T = K \cdot \delta t$ can be formulated as $\mathbf{Z}_T = [\mathbf{A}^{(\delta t)}]^K\mathbf{X}$. Adjusting δt enables smoother propagation rate modulation, mitigating representation instability in discrete propagation.

Graph Diffusion Augmentation. Indeed, deterministic diffusion states capture specific graph spectral responses. To eliminate architectural bias, the condensed graph should maintain state consistency with the original graph for arbitrary diffusion times to inherit the complete spectral properties.

As a sample generation strategy, data augmentation [10, 29] aims to enhance the generalizability and robustness of the model through diverse samples. Inspired by this, a simple yet efficient diffusion augmentation is proposed to improve the generalizability of the condensed graph by generating diverse diffusion states with hybrid intervals. This process can be formulated as:

$$\mathcal{S}(\mathbf{Z}_T^\tau) = \left\{\mathbf{Z}_T^\tau \mid \mathbf{Z}_T^\tau = [\mathbf{A}^{(\delta t_\tau)}]^K\mathbf{X},\ \delta t_\tau \sim \mathcal{P},\ \forall \delta t_\tau \leq \frac{2}{\lambda_{\max}(\mathbf{L})}\right\}_{\tau=0}^{\mathcal{T}} \tag{6}$$

where $\mathcal{P} = \mathcal{U}(\delta t_{\min}, 2/\lambda_{\max}(\mathbf{L})))$, $\mathcal{T}$ denotes the condensation epoch, and $\lambda_{\max}(\mathbf{L})$ is the maximum eigenvalue of $\mathbf{L}$. $\forall \delta t_\tau \leq 2/\lambda_{\max}(\mathbf{L})$ ensures the stability of the graph diffusion. Similarly, $\mathcal{S}(\tilde{\mathbf{Z}}_T^\tau)$ is obtained by keeping the same δt_τ as above on $\tilde{\mathcal{G}}$.

It can be seen from Eq. (6) that the stochastic variation of the diffusion interval δt raises uncertainty of the diffusion state at time T. By aligning the two graph representations $\mathbf{Z}_T^\tau$ and $\tilde{\mathbf{Z}}_T^\tau$, the condensed graph is guided to capture the diffusion trajectories of the original graph across varying states. In addition, we can derive the following proposition (Proofs are in Appendix A):

Proposition 4.1. *When enough diffusion times $\{\delta t_\tau\}_{\tau=1}^{\mathcal{T}}$ are sampled from the distribution $\mathcal{P}$ over the interval $I = [\delta t_{\min}, 2/\lambda_{\max}(\mathbf{L})]$, the spectral response function is satisfied by sampling coverage over the entire spectral range:*

$$\lim_{\mathcal{T}\to\infty} \Pr(\max_i \sup_{\delta t\in I} \min_\tau |\Phi_i(\delta t) - \Phi_i(\delta t_\tau)| < \varphi) = 1,\ \forall \varphi > 0 \tag{7}$$

where $\Phi_i(\delta t) = e^{-K\delta t\lambda_i}$ is the spectral response function for the i-th eigenvalue λ_i.

Proposition 4.1 establishes a fundamental probabilistic guarantee for the completeness of spectral coverage in graph diffusion augmentation. This strategy breaks through the fixed-architecture constraints in conventional GC methods and effectively preserves the original spectral properties.

4.2 Optimal Transport Plan Matching

For the generalized GC objective in Eq. (4), the distance function $\Delta_{\mathcal{Y}}(\cdot,\cdot)$ is challenging to define without any task signal. However, semantic information should be an intrinsic property of the graph, rather than being influenced by the downstream task. In other words, the semantics of the same node should remain unchanged in both the graph and the representation spaces. This insight inspired us to ensure the consistency of semantic associations between $\mathcal{G}$ and $\tilde{\mathcal{G}}$ by defining two similarity metrics in graph and representation spaces, respectively. In fact, it is nontrivial to directly compare these two metrics, since they belong to two different spaces and are two disjoint objects by nature.

Fortunately, optimal transport theory provides an elegant framework for this purpose. Therefore, we present an optimal transport plan matching, which aims to find the consistent optimal plan for graph alignment and representation alignment. For the graph space, a natural idea is to consider both node features and structure information in the transport plan. In PreGC, the fused Gromov-Wasserstein [43] is adopted to obtain the optimal transport plan $\pi_{\mathcal{D}}^* \in \mathbb{R}^{N\times M}$:

$$\pi_{\mathcal{D}}^*(\mathcal{G},\tilde{\mathcal{G}}) = \underset{\pi_{\mathcal{D}}\in\Pi(\mu,\nu)}{\arg\min} \left\langle \gamma\boldsymbol{\mathcal{K}}(\mathbf{X},\tilde{\mathbf{X}}) + (1-\gamma)\boldsymbol{\mathcal{J}}(\mathbf{A},\tilde{\mathbf{A}}) \otimes \pi_{\mathcal{D}}, \pi_{\mathcal{D}} \right\rangle \tag{8}$$

where $\otimes$ denotes the tensor-matrix multiplication, and γ represents the coefficient used to control the importance of structure and features. $\boldsymbol{\mathcal{K}}(\mathbf{X}, \tilde{\mathbf{X}})_{i,j} = \|\mathbf{X}_i - \tilde{\mathbf{X}}_j\|_2$ and $\boldsymbol{\mathcal{J}}(\mathbf{A}, \tilde{\mathbf{A}})_{ij,kl} = |\mathbf{A}_{ik} - \tilde{\mathbf{A}}_{jl}|$ are cost metric functions that measure feature discrepancy and structure discrepancy, respectively. For the node presentation, we leverage Wasserstein distance to obtain the optimal plan $\pi^*_{\mathcal{Z}} \in \mathbb{R}^{N \times M}$:

$$\pi^*_{\mathcal{Z}}(\mathbf{Z}^\tau_T, \tilde{\mathbf{Z}}^\tau_T) = \underset{\pi_{\mathcal{Z}} \in \Pi(\mu,\nu)}{\arg\min} \left\langle \boldsymbol{\mathcal{K}}(\mathbf{Z}^\tau_T, \tilde{\mathbf{Z}}^\tau_T), \pi_{\mathcal{Z}} \right\rangle \tag{9}$$

Intuitively, the optimal transport plan characterizes the transferring probability from source nodes to condensed nodes, and semantic association consistency in different spaces is preserved by minimizing the divergence between two transport plans. The transport plan matching loss is defined as follows:

$$\mathcal{L}_{plan} = \Delta_{\mathcal{Y}}\big(\pi^*_{\mathcal{D}}(\mathcal{G}, \tilde{\mathcal{G}}), \pi^*_{\mathcal{Z}}(\mathbf{Z}^\tau_T, \tilde{\mathbf{Z}}^\tau_T)\big) \tag{10}$$

Without loss of generality, $\Delta_{\mathcal{Y}}(\cdot, \cdot)$ is set to the Frobenius norm in this paper.

4.3 Node Significance Evaluation

Unlike conventional GC works without explicittly considering node contributions for condensation, the optimal resresentation transport plan $\pi^*_{\mathcal{Z}}$ here not only delineates the semantic associations between both graphs, but also inversely reflects the potential significance of the source nodes. Specifically, let's first define a mask matrix $\pi_{mask} \in \mathbb{R}^{N \times M}$ to filter out the most influencial nodes from source graph $\mathcal{G}$ on each condensed node j , i.e., we have $(\pi_{mask})_{i,j} = (\pi^*_{\mathcal{Z}})_{i,j}$ when $(\pi^*_{\mathcal{Z}})_{i,j}$ is among the top-H of the j-th column, otherwise $(\pi_{mask})_{i,j} = 0$. Then, the node significance score vector $\mathbf{s} \in \mathbb{R}^N$ of the source graph can be obtained by:

$$\mathbf{s} = \pi_{mask} \cdot \mathbf{1}_M \tag{11}$$

where $\mathbf{1}_M \in \mathbb{R}^M$ denotes the all-ones vector. Essentially, the significance $\mathbf{s}$ explicitly reveals the contributions of different source nodes for the condensed graph. Noticeably, the evaluation of node significance based on $\mathbf{s}$ are two-folds. On the one hand, it provides more transparent interpretability for graph condensation, and on the other hand, it also helps to guide node labeling effectively in an active learning way [20]. Section 5.2 further confirms the validity of the node significance evaluation.

4.4 Condensed Graph Optimization

Pre-training. Benefiting from Eq. (9), the reconstruction term $\mathcal{O}_{\mathcal{Z}}$ can be achieved by diffusion alignment between $\mathbf{Z}^\tau_T$ and $\tilde{\mathbf{Z}}^\tau_T$. Therefore, according to Eq. (4), the total loss can be denoted as:

$$\mathcal{L}_{total} = \mathcal{L}_{cost} + \xi \mathcal{L}_{plan}, \quad \mathcal{L}_{cost} = \Delta_{\mathcal{Z}}(\mathbf{Z}^\tau_T, \tilde{\mathbf{Z}}^\tau_T) \tag{12}$$

where $\Delta_{\mathcal{Z}}(\cdot, \cdot)$ denotes the Wasserstein distance [39]. After obtaining the condensed graph $\tilde{\mathcal{G}}$, the transport plan $\pi^*_{\mathcal{Z}}$, which reflects the transfer probabilities between the source nodes from $\mathcal{G}$ and the condensed nodes, is also retained. To ensure the uniqueness of the semantic mapping, we discretize $\pi^*_{\mathcal{Z}}$ to obtain the semantic assignment matrix $\mathbf{M} \in \mathbb{R}^{N \times M}$:

$$\mathbf{M}_{i,j} = \mathbb{I}(j = \underset{1 \le l \le M}{\arg\max} (\pi^*_{\mathcal{Z}})_{i,l}) \tag{13}$$

When the condensed graph $\tilde{\mathcal{G}}$ needs to be trained on downstream tasks, the target variable $\tilde{\mathbf{Y}} \in \mathbb{R}^{M \times C}$ can be obtained from the original label by the traceable semantic harmonizer $\boldsymbol{\mathcal{M}}_{\mathcal{Z}}(\cdot)$:

$$\tilde{\mathbf{Y}} = \boldsymbol{\mathcal{M}}_{\mathcal{Z}}(\mathbf{Y}_{tr}) = \mathbf{D}^{-1}_{\Omega} \mathbf{M}^\top_{\Omega} \mathbf{Y}_{tr} \tag{14}$$

where $\mathbf{Y}_{tr} \in \mathbb{R}^{N_{tr} \times C}$ is a training label with N_{tr} labelled nodes, and $\Omega = \{i_1, ..., i_{N_{tr}}\}$ is the set of their row indices. $\mathbf{M}_{\Omega} \in \mathbb{R}^{N_{tr} \times M}$ denotes the sub-assignment matrix defined by $(\mathbf{M}_{\Omega})_{k,j} = \mathbf{M}_{i_k,j}$. $\mathbf{D}_{\Omega} = \text{diag}(\mathbf{M}^\top_{\Omega} \mathbf{1}_{N_{tr}}) \in \mathbb{R}^{M \times M}$, and $\text{diag}(\cdot)$ is used to create a diagonal matrix.

Test Time Fine-tuning. To further unlock the potential of condensed graphs while improving the performance of condensed graphs on different tasks and GNN architectures, we draw on the idea of fine-tuning pre-trained models [3] to propose PreGC$_{\text{ft}}$, a strategy for achieving finer semantic alignment by fine-tuning the assignment matrix. Specifically, given a decay rate $\epsilon \in [0, 1]$, the assignment matrix $\mathbf{M}$ is updated every τ_{up} epochs according to predefined tasks and GNN:

$$\mathbf{M} \leftarrow \epsilon \mathbf{M} + (1 - \epsilon) \mathbf{M}_{up} \tag{15}$$

where $\mathbf{M}_{up} \in \mathbb{R}^{N \times M}$ is obtained from $\tilde{\pi}^*_{\mathcal{Y}}(\hat{\mathbf{Y}}, \hat{\tilde{\mathbf{Y}}})$ similar as Eq. (9). $\hat{\mathbf{Y}}$ and $\hat{\tilde{\mathbf{Y}}}$ are the predicted outputs by the specific GNN encoded from $\mathcal{G}$ and $\tilde{\mathcal{G}}$, respectively.

Through the above optimization framework, we empower GC with pre-training and fine-tuning capabilities. The overall pipeline of PreGC are summarized in Appendix B.

5 Experiments

5.1 Experimental Settings

Datasets. To comprehensively evaluate the condensation performance of PreGC, five graph datasets (Cora, Citeseer, Pubmed [26], OGB-Arxiv [60], and H&M [2]) are utilized in experiments. Different tasks are tested to validate the generalization of PreGC, including node classification (NC), node clustering (NClu), link prediction (LP), and node regression (NR). Specifically, OGB-Arxiv includes two NC tasks: predicting paper topics (T) and publication years (Y). H&M includes an NC task: predicting product categories (C), and an NR task: predicting product prices (P). Two condensation ratios ($r = \frac{M}{N}$) are considered. More details are provided in Appendix C.1.

Baselines & Implementations. We compare the proposed PreGC with six representative graph condensation methods (GCDM [32], GCond [25], SFGC [64], SGDD [55], GDEM [33], and CGC [16]). Following [25, 42], the condensed graph is synthesized according to the default settings of the above methods, and a certain GNN (default is SGC [48]) is trained on this graph and evaluated on the test set of the original graph. Moreover, other eight representative GNNs (GCN [26], APPNP [27], k-GNN [38], GAT [44], GraphSAGE [19], SSGC [65], BernNet [23], and GPRGNN [8]) are selected to evaluate the effectiveness of PreGC. The details of baselines, task settings, condensation settings, and parameter settings are provided in Appendix C.2 and C.3.

Table 1: Performance comparison on different tasks (We report test accuracy (%) on NC, NMI (%) on NClu, and AUC (%) on LP tasks. **Bold entry** is the best result, underline marks the runner-up).

Dataset	Task	Ratio	GCDM (2022)	GCond (2022)	SFGC (2023)	SGDD (2023)	GDEM (2024)	CGC (2025)	PreGC (Our)	Whole
Cora	NC	1.3%	61.5±1.2	79.0±1.3	75.4±0.5	79.2±0.6	80.8±0.4	79.0±0.8	**81.1±0.3**	80.8±0.8
		2.6%	69.2±0.4	79.0±0.6	79.2±1.4	81.1±0.8	80.7±0.1	**81.8±0.6**	81.6±0.9	
	NC→NClu	1.3%	36.9±0.7	58.1±1.6	56.0±2.0	**59.0±1.2**	57.2±0.8	58.2±1.2	54.6±1.0	59.3±1.5
		2.6%	45.3±0.5	57.6±0.9	57.3±0.7	58.7±0.5	57.0±0.5	59.4±0.5	**59.6±0.5**	
	LP	1.3%	56.8±0.7	56.6±3.0	N/A	57.0±3.5	66.9±0.6	65.5±0.8	**75.3±2.2**	81.9±4.8
		2.6%	57.2±1.8	62.2±1.6	N/A	60.4±2.2	59.7±2.6	46.5±4.1	**79.2±2.2**	
	LP→NClu	1.3%	19.1±4.7	26.8±10.1	N/A	14.3±6.6	29.5±3.8	8.9±0.7	**33.6±1.0**	42.3±3.3
		2.6%	13.1±2.8	32.0±6.0	N/A	13.4±3.3	**35.2±1.4**	10.3±1.9	34.9±2.1	
Citeseer	NC	0.9%	54.7±1.2	68.9±1.0	67.1±0.9	68.9±1.6	**70.6±0.3**	70.5±0.4	**70.6±0.5**	69.2±0.4
		1.8%	52.1±0.9	67.9±0.7	65.1±1.5	69.7±1.7	70.5±0.4	70.6±0.4	**70.8±0.8**	
	NC→NClu	0.9%	25.3±0.7	41.0±2.7	42.4±1.8	43.0±1.3	42.8±0.7	40.6±1.7	**43.8±1.4**	42.4±0.5
		1.8%	20.8±2.5	38.1±0.8	42.9±0.9	43.5±0.7	**45.2±0.4**	40.7±1.8	43.9±0.6	
	LP	0.9%	61.5±3.8	61.5±2.0	N/A	60.0±2.2	65.8±3.7	N/A	**66.5±1.6**	80.8±4.9
		1.8%	57.5±5.3	62.3±3.4	N/A	56.9±2.7	64.3±3.6	55.5±3.9	**69.3±3.3**	
	LP→NClu	0.9%	7.2±0.9	20.3±3.3	N/A	10.1±1.2	21.0±2.5	N/A	**32.7±0.7**	33.4±3.8
		1.8%	9.3±3.0	14.7±3.0	N/A	9.2±1.4	16.9±3.3	7.2±1.4	**33.1±1.2**	
Pubmed	NC	0.08%	71.4±1.6	72.9±0.6	77.4±0.2	78.4±0.4	77.8±0.1	78.7±0.3	**79.9±0.4**	78.8±0.2
		0.15%	60.8±0.8	71.6±1.4	78.1±0.4	78.6±0.5	76.8±0.6	78.4±0.5	**81.0±0.5**	
	NC→NClu	0.08%	24.8±2.8	21.1±5.5	35.3±0.6	35.6±0.8	35.5±0.1	**37.0±0.6**	35.6±0.8	37.1±0.8
		0.15%	19.4±0.5	18.9±0.7	36.9±0.2	36.1±0.3	34.1±0.4	38.0±0.4	**38.3±0.7**	
	LP	0.08%	72.1±2.9	72.9±3.8	N/A	72.9±3.1	43.5±1.6	N/A	**82.9±2.0**	95.0±1.0
		0.15%	68.9±4.2	73.7±3.5	N/A	68.4±3.2	56.1±2.3	84.8±2.0	**86.3±2.4**	
	LP→NClu	0.08%	14.1±3.0	6.2±4.4	N/A	3.0±0.4	1.6±0.2	N/A	**22.5±0.7**	30.7±3.3
		0.15%	13.7±0.4	4.1±1.8	N/A	12.0±1.8	20.1±4.2	23.5±0.3	**24.0±1.0**	

5.2 Experimental Results

Performance of PreGC on Various Tasks. We first demonstrate the generalizability of the condensed graph obtained by PreGC as shown in Table 1. Clearly, PreGC achieves optimal performance in most cases. In particular, PreGC consistently outperforms baselines on LP, demonstrating that the condensed graph of PreGC can well capture the topological relationships in the original structure. SFGC is unable to perform LP task (i.e. "N/A") due to its emphasis on structure-free during

condensation, limiting its task reusability. In addition, Table 2 shows the generalization of PreGC under different supervision tasks and the flexibility in task migration. Owing to the limitations that need to initialize condensed labels by the original class labels, existing methods can't be directly applied to node regression (i.e. "N/A"). By virtue of its unsupervised matching strategy, PreGC becomes the first GC method capable of adapting to NR task. Regardless of the tasks, PreGC consistently achieved optimal performance. In addition, the fine-tuning strategy PreGC_{ft} achieves 1.46% gain compared to PreGC on H&M dataset.

Table 2: Performance comparison to baselines on different supervised tasks ("Y→T" means condensation on the "Y" task and testing on the "T" task. We report test accuracy (%) on NC and R^2 (%) on NR tasks. **Imp.** indicates the performance improvement over the best baseline).

	OGB-Arxiv ($r = 1.25\%$)				H&M ($r = 2.5\%$)			
	T→T	Y→T	Y→Y	T→Y	C→C	P→C	P→P	C→P
Whole	64.43 ± 0.24		55.37 ± 0.21		77.07 ± 0.26		50.80 ± 0.64	
GCDM	33.08±1.04	46.48±2.40	44.20±0.84	46.17±1.25	57.15±0.90	N/A	N/A	26.08±0.76
GCond	56.74±0.65	41.38±1.65	49.25±0.67	42.52±2.12	64.57±0.53	N/A	N/A	15.29±1.14
SFGC	59.64±0.22	50.15±1.55	50.07±0.47	44.30±1.76	60.09±1.24	N/A	N/A	4.81±1.04
SGDD	58.68±0.82	27.80±2.09	41.70±2.25	42.30±1.58	61.85±0.39	N/A	N/A	18.85±2.13
GDEM	53.93±0.71	40.01±0.87	49.17±0.32	47.80±0.96	52.61±3.05	N/A	N/A	6.83±2.99
CGC	58.71±0.65	53.32±1.61	49.50±0.72	48.53±0.24	64.35±0.33	N/A	N/A	15.95±1.11
PreGC	60.55±0.43	59.62±0.47	52.34±0.30	51.49±0.36	69.06±0.25	68.86±0.29	34.39±0.93	33.17±1.05
Imp.	0.91↑	6.30↑	2.84↑	2.96↑	4.49↑	-	-	7.09↑
PreGC_{ft}	**60.81±0.40**	**60.86±0.43**	**52.47±0.20**	**52.41±0.25**	**69.98±0.24**	**69.98±0.28**	**34.75±0.74**	**34.63±0.69**
Imp.	1.17↑	7.54↑	2.97↑	3.88↑	5.41↑	-	-	8.55↑

Generalizability of PreGC across Different GNNs. Ideal condensed graphs should perform well in different GNNs, and to this end, each synthetic graph is evaluated by nine GNNs, and the results are shown in Table 3. It is evident that the PreGC exhibits the highest average accuracy, suggesting that the condensed graph extracted by PreGC can consistently benefit various GNNs. Furthermore, only SFGC and PreGC have average accuracy exceeding that of training on the raw graph. However, SFGC can lead to limited application scenarios due to its lack of explicit structure.

Table 3: Node classification performance across different GNNs on Pubmed ($r = 0.15\%$). Highlight marks the lossless results and **Avg.** is the average results of GNNs.

	SGC	GCN	APPNP	k-GNN	GAT	SAGE	SSGC	Bern.	GPR.	**Avg.**
Whole	78.9±0.2	78.2±0.4	79.2±0.4	77.0±0.8	77.2±0.4	77.0±0.5	79.0±0.3	77.4±0.5	79.0±0.3	78.1±1.0
GCDM	60.8±0.8	56.8±1.1	70.0±0.9	72.3±0.5	76.2±0.8	53.3±0.8	69.8±0.4	68.2±1.3	71.1±0.7	66.5±7.7
GCond	71.6±1.6	73.1±1.7	73.0±0.2	65.9±2.4	71.7±2.9	69.4±1.5	73.3±0.4	72.6±2.2	72.4±0.8	71.4±2.4
SFGC	78.1±0.4	78.9±0.7	79.7±0.6	78.1±0.7	77.5±0.8	75.9±0.5	78.7±0.3	78.4±0.4	79.0±0.2	78.3±1.1
SGDD	78.6±0.5	78.7±0.3	78.7±0.7	76.7±0.7	73.4±3.0	76.4±0.4	78.6±0.2	77.3±0.5	77.4±0.7	77.3±1.7
GDEM	76.8±0.6	77.3±0.3	77.7±0.4	78.2±0.5	76.7±0.7	76.4±1.3	77.5±1.1	76.9±0.4	77.0±0.3	77.2±0.6
CGC	78.4±0.5	79.5±0.3	78.8±0.4	75.7±0.9	**78.9±0.5**	76.4±0.7	79.0±0.4	77.3±0.4	78.5±0.6	78.1±1.3
PreGC	**81.0±0.5**	**80.3±0.4**	**80.9±0.3**	**79.1±0.5**	77.8±1.0	**77.9±1.0**	**81.3±0.4**	**80.2±0.3**	**80.0±0.5**	**79.8±1.3**

Performance Gap between Condensed Graph and Original Graph. According to [16, 49, 33], the quality of condensed graphs can be quantified through class-level features on NC task. Therefore, we present the labeled reconstruction error $LRE = \frac{1}{K}\sum_{k=0}^{K} \|\mathbf{Y}^\dagger \mathbf{A}^k \mathbf{X} - \tilde{\mathbf{Y}}^\dagger \tilde{\mathbf{A}}^k \tilde{\mathbf{X}}\|_F$ with the class label to evaluate condensed graphs. This formulation systematically captures multiscale receptive fields through the expectation over propagation steps to evaluate the distribution discrepancy. We set $K = 5$ and the case $k = 0$ is also taken into account, which reflects the difference between the condensed and original features. As shown in Fig. 3, compared with two representative GC methods [16, 33], the LRE of PreGC is consistently lower than that of the other two methods on different data and tasks. Since PreGC does not use any task labels in condensation, this is more challenging than baselines and also demonstrates the effectiveness of traceable semantic harmonizer.

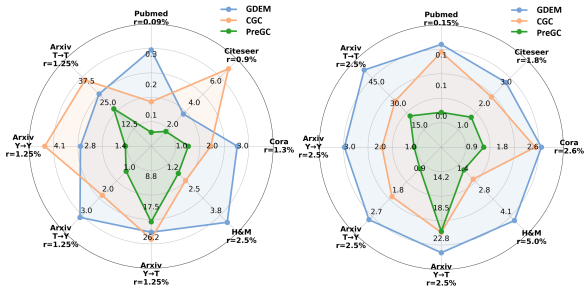

Figure 3: The LRE of different GC methods.

Data Valuation based on Node Significance. To confirm the validity of the significance evaluation in Section 4.3, we rescreened the same number of nodes as the original training set based on Eq. (11) and retrained them on the original graph. Fig. 4 (b) shows a visualization of the distribution of nodes in the rescreened training set (Dark nodes denote the training set, and distinct colors denote different classes). Compared to the default training set provided by [26] (Fig. 4 (a)), the rescreened training set demonstrates greater coverage and distributional dispersion. We further measure distribution differences with the average nearest neighbor distance $\bar{d} = \frac{1}{|\mathcal{V}_{tr}|}\sum_{i\in\mathcal{V}_{tr}}\min_{j\neq i}\|\mathbf{z}_i - \mathbf{z}_j\|_2$ (larger $\bar{d}$ indicates wider coverage of the selected labels, and 2-order diffusion is considered, i.e., $\mathbf{Z} = \mathbf{A}^2\mathbf{X}$ by default), and the results also confirmed the above viewpoint. Fig. 4 (c) compares the performance of SGC trained with different training sets. Leveraging the rescreened nodes as supervision yields higher classification accuracy and markedly improves the training efficiency of the source graph.

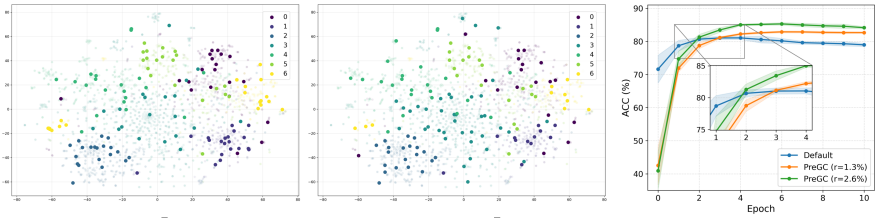

(a) Default ($\bar{d}$ = 1.66) (b) PreGC-2.6% ($\bar{d}$ = 1.79) (c) Performance on Cora

Figure 4: Performance of the training set selected via node significance on Cora.

Table 4: The prerformance of GC mehtods with different trainig ratio on OGB-Arxiv.

Training Ratio	0.15	0.3	0.45	0.6	0.75	Count
Whole	66.71±0.43	69.53±0.11	70.44±0.51	71.69±0.20	71.72±0.57	-
GCDM	35.98±1.31	36.32±1.08	36.09±0.89	36.94±0.60	38.35±0.67	×5
GCond	56.17±0.30	56.95±0.31	56.83±0.49	57.47±0.36	58.00±0.34	×5
SFGC	59.09±0.42	59.85±0.38	60.04±0.53	60.46±0.51	60.59±0.48	×5
SGDD	58.01±0.77	58.79±0.40	59.03±0.44	59.54±0.53	60.24±0.46	×5
GDEM	52.23±0.32	54.20±0.57	54.81±0.44	54.98±0.48	55.41±0.31	×5
CGC	58.39±0.33	59.04±0.49	58.92±0.72	59.53±0.56	60.05±0.29	×5
PreGC	**60.53±0.32**	**61.96±0.56**	**61.72±0.63**	**63.37±0.49**	**63.58±0.82**	**×1**

Flexibility of PreGC. The existing condensation methods are limited to concentrating under certain proportions of labels. When new labels are added in the original graph, these methods must re-condensation to capture this new knowledge in the condensed graph, which undoubtedly increases the condensation cost and limits its flexibility. PreGC can quickly transfer new labels to the condensed graph through the traceable semantic harmonizer without re-condensation. As shown in Table 4, we rescaled the training set ratio of the original graph and recorded the number of re-condensation (Count). With the structure and features of the condensed graph fixed, the condensed graph by PreGC shows similar patterns of change as the original graph as the training ratio increases. This label allocation strategy significantly improves the reusability of PreGC. Notably, existing baselines require repeated re-condensation to incorporate new label knowledge ($\times 5$), whereas PreGC achieves this with a single pass of semantic assignment matrix $\mathbf{M}$.

Ablation Study. To validate the efficacy of crucial optimization strategies, we conduct a comprehensive analysis on H&M dataset through ablation studies. The experimental results are shown in Table 5, wherein "PreGC$_{\text{w/o } Aug}$" is the PreGC that removes the graph diffusion augmentation and "PreGC$_{\text{w/o } \mathcal{L}_{cost}}$" is the adoption of the existing strategy, i.e. predefined node labels before GC. We observe that both graph diffusion augmentation and $\mathcal{L}_{cost}$ contribute significantly to the improvement of the GC optimization. Notably, "PreGC$_{\text{w/o } \mathcal{L}_{cost}}$" induces label dependency in condensation, rendering the condensed graph via category prove inadequate for achieving superior performance on price prediction. Furthermore, the combination of these two modules increases the stability of the condensed graph.

Table 5: Experimental results for the ablation study.

H&M	$r = 2.5\%$		$r = 5.0\%$	
	Category	Price	Category	Price
PreGC	69.1±0.3	34.4±0.9	71.1±0.3	36.9±1.1
PreGC$_{\text{w/o } Aug}$	66.6±0.7	32.2±0.9	67.9±0.4	33.3±1.4
PreGC$_{\text{w/o } \mathcal{L}_{cost}}$	67.5±0.5	29.1±0.8	68.9±0.8	31.7±1.5

More experimental analysis, including generalizability of PGC across different GNNs, comparison of LRE with different GC methods, data valuation, and sensitivity analysis are detailed in Appendix D. In addition, we also discuss the related work and limitations in Appendix E.

6 Conclusions

In this work, we revisit the limitations of current GC methods and formulate a generalized GC objective. Following this paradigm, we further propose a pre-trained graph condensation framework for distilling a task-agnostic and architecture-flexible condensed graph. To avoid excessive dependence of condensed graphs on specific GNNs, a hybrid-interval graph diffusion augmentation is proposed to enhance generalization by increasing node state uncertainty. Subsequently, a plan matching mechanism is derived to eliminate task constraints, which relies on matching optimal transport plans for graph alignment and representation alignment to preserve semantic association consistency. In addition, supervised fine-tuning further refines the condensed task signals and improves the performance of the condensed graph on specific tasks. The experimental results consistently demonstrate the efficacy and reusability of PreGC, showcasing its generalization on various GNNs and tasks.

Acknowledgments and Disclosure of Funding

This work was supported in part by the National Key Research and Development Program of China (2024YFF0505704), National Natural Science Foundation of China (62476022, 62506029), Beijing Natural Science Foundation (L251043, 4254085), and China Postdoctoral Science Foundation (2025M771589). The authors would also like to thank the anonymous reviewers for their constructive comments and valuable suggestions on this paper.

References

[1] Joshua D. Batson, Daniel A. Spielman, and Nikhil Srivastava. Twice-ramanujan sparsifiers. In *ACM Symposium on Theory of Computing (STOC)*, pages 255–262, 2009.

[2] Gleb Bazhenov, Oleg Platonov, and Liudmila Prokhorenkova. Tabgraphs: A benchmark and strong baselines for learning on graphs with tabular node features. *arXiv preprint arXiv: 2409.14500*, 2024.

[3] Ju-Seung Byun, Jiyun Chun, Jihyung Kil, and Andrew Perrault. ARES: alternating reinforcement learning and supervised fine-tuning for enhanced multi-modal chain-of-thought reasoning through diverse AI feedback. In *Empirical Methods in Natural Language Processing (EMNLP)*, pages 4410–4430, 2024.

[4] Dong Chen, Shuai Zheng, Yeyu Yan, Muhao Xu, Zhenfeng Zhu, Yao Zhao, and Kunlun He. Dynamic graph condensation. *arXiv preprint arXiv:2506.13099*, 2025.

[5] Hao Chen, Yuanchen Bei, Qijie Shen, Yue Xu, Sheng Zhou, Wenbing Huang, Feiran Huang, Senzhang Wang, and Xiao Huang. Macro graph neural networks for online billion-scale recommender systems. In *the ACM on Web Conference (WWW)*, pages 3598–3608, 2024.

[6] Liqun Chen, Zhe Gan, Yu Cheng, Linjie Li, Lawrence Carin, and Jingjing Liu. Graph optimal transport for cross-domain alignment. In *International Conference on Machine Learning (ICML)*, volume 119, pages 1542–1553, 2020.

[7] Tianlong Chen, Yongduo Sui, Xuxi Chen, Aston Zhang, and Zhangyang Wang. A unified lottery ticket hypothesis for graph neural networks. In *International Conference on Machine Learning (ICML)*, volume 139, pages 1695–1706, 2021.

[8] Eli Chien, Jianhao Peng, Pan Li, and Olgica Milenkovic. Adaptive universal generalized pagerank graph neural network. In *International Conference on Learning Representations (ICLR)*, 2021.

[9] Fan RK Chung. *Spectral graph theory*, volume 92. American Mathematical Soc., 1997.

[10] Jinhao Cui, Heyan Chai, Xu Yang, Ye Ding, Binxing Fang, and Qing Liao. SGCL: semantic-aware graph contrastive learning with lipschitz graph augmentation. In *IEEE International Conference on Data Engineering (ICDE)*, pages 3028–3041, 2024.

[11] M Cuturi. Lightspeed computation of optimal transportation distances. *Neural Information Processing Systems (NeurIPS)*, 26(2):2292–2300, 2013.

[12] Matthias Fey, Weihua Hu, Kexin Huang, Jan Eric Lenssen, Rishabh Ranjan, Joshua Robinson, Rex Ying, Jiaxuan You, and Jure Leskovec. Position: Relational deep learning - graph representation learning on relational databases. In *International Conference on Machine Learning (ICML)*, 2024.

[13] Jian Gao, Jianshe Wu, and Jingyi Ding. Heterogeneous graph condensation. *IEEE Trans. Knowl. Data Eng.*, 36(7):3126–3138, 2024.

[14] Xinyi Gao, Tong Chen, Yilong Zang, Wentao Zhang, Quoc Viet Hung Nguyen, Kai Zheng, and Hongzhi Yin. Graph condensation for inductive node representation learning. In *International Conference on Data Engineering (ICDE)*, pages 3056–3069, 2024.

[15] Xinyi Gao, Yayong Li, Tong Chen, Guanhua Ye, Wentao Zhang, and Hongzhi Yin. Contrastive graph condensation: Advancing data versatility through self-supervised learning. *arXiv preprint arXiv: 2411.17063*, 2024.

[16] Xinyi Gao, Guanhua Ye, Tong Chen, Wentao Zhang, Junliang Yu, and Hongzhi Yin. Rethinking and accelerating graph condensation: A training-free approach with class partition. In *The ACM Web Conference (WWW)*, 2025.

[17] Mridul Gupta, Samyak Jain, Vansh Ramani, Hariprasad Kodamana, and Sayan Ranu. Bonsai: Gradient-free graph distillation for node classification. *arXiv preprint arXiv:2410.17579*, 2024.

[18] Mridul Gupta, Sahil Manchanda, Hariprasad Kodamana, and Sayan Ranu. Mirage: Model-agnostic graph distillation for graph classification. *arXiv preprint arXiv:2310.09486*, 2023.

[19] William L. Hamilton, Zhitao Ying, and Jure Leskovec. Inductive representation learning on large graphs. In *Neural Information Processing Systems (NeurIPS)*, pages 1024–1034, 2017.

[20] Haoyu Han, Xiaorui Liu, Li Ma, MohamadAli Torkamani, Hui Liu, Jiliang Tang, and Makoto Yamada. Structural fairness-aware active learning for graph neural networks. In *International Conference on Learning Representations (ICLR)*, 2024.

[21] Xiaoxue Han, Zhuo Feng, and Yue Ning. A topology-aware graph coarsening framework for continual graph learning. In *Neural Information Processing Systems (NeurIPS)*, 2024.

[22] Mohammad Hashemi, Shengbo Gong, Juntong Ni, Wenqi Fan, B. Aditya Prakash, and Wei Jin. A comprehensive survey on graph reduction: Sparsification, coarsening, and condensation. In *International Joint Conference on Artificial Intelligence (IJCAI)*, pages 8058–8066, 2024.

[23] Mingguo He, Zhewei Wei, Zengfeng Huang, and Hongteng Xu. Bernnet: Learning arbitrary graph spectral filters via bernstein approximation. In *Neural Information Processing Systems (NeurIPS)*, pages 14239–14251, 2021.

[24] Wei Jin, Xianfeng Tang, Haoming Jiang, Zheng Li, Danqing Zhang, Jiliang Tang, and Bing Yin. Condensing graphs via one-step gradient matching. In *Knowledge Discovery and Data Mining (KDD)*, pages 720–730, 2022.

[25] Wei Jin, Lingxiao Zhao, Shichang Zhang, Yozen Liu, Jiliang Tang, and Neil Shah. Graph condensation for graph neural networks. In *International Conference on Learning Representations (ICLR)*, 2022.

[26] Thomas N. Kipf and Max Welling. Semi-supervised classification with graph convolutional networks. In *International Conference on Learning Representations (ICLR)*, 2017.

[27] Johannes Klicpera, Aleksandar Bojchevski, and Stephan Günnemann. Predict then propagate: Graph neural networks meet personalized pagerank. In *International Conference on Learning Representations (ICLR)*, 2019.

[28] Manoj Kumar, Anurag Sharma, Shashwat Saxena, and Sandeep Kumar. Featured graph coarsening with similarity guarantees. In *International Conference on Machine Learning (ICML)*, volume 202, pages 17953–17975, 2023.

[29] Chao Li, Xinming Liu, Yeyu Yan, Zhongying Zhao, and Qingtian Zeng. Hetgnn-sf: Self-supervised learning on heterogeneous graph neural network via semantic strength and feature similarity. *Appl. Intell.*, 53(19):21902–21919, 2023.

[30] Xunkai Li, Yinlin Zhu, Boyang Pang, Guochen Yan, Yeyu Yan, Zening Li, Zhengyu Wu, Wentao Zhang, Rong-Hua Li, and Guoren Wang. Openfgl: A comprehensive benchmarks for federated graph learning. *arXiv preprint arXiv: 2408.16288*, 2024.

[31] Yibo Li, Xiao Wang, Hongrui Liu, and Chuan Shi. A generalized neural diffusion framework on graphs. In *AAAI Conference on Artificial Intelligence (AAAI)*, pages 8707–8715, 2024.

[32] Mengyang Liu, Shanchuan Li, Xinshi Chen, and Le Song. Graph condensation via receptive field distribution matching. *arXiv preprint arXiv:2206.13697*, 2022.

[33] Yang Liu, Deyu Bo, and Chuan Shi. Graph distillation with eigenbasis matching. In *International Conference on Machine Learning (ICML)*, 2024.

[34] Yilun Liu, Ruihong Qiu, and Zi Huang. Cat: Balanced continual graph learning with graph condensation. In *IEEE International Conference on Data Mining (ICDM)*, pages 1157–1162, 2023.

[35] Yilun Liu, Ruihong Qiu, and Zi Huang. Cat: Balanced continual graph learning with graph condensation. In *IEEE International Conference on Data Mining (ICDM)*, pages 1157–1162, 2023.

[36] Yilun Liu, Ruihong Qiu, Yanran Tang, Hongzhi Yin, and Zi Huang. Puma: Efficient continual graph learning with graph condensation. *arXiv preprint arXiv:2312.14439*, 2(4), 2023.

[37] Weigang Lu, Ziyu Guan, Wei Zhao, and Yaming Yang. Adagmlp: Adaboosting gnn-to-mlp knowledge distillation. In *Knowledge Discovery and Data Mining (KDD)*, pages 2060–2071, 2024.

[38] Christopher Morris, Martin Ritzert, Matthias Fey, William L. Hamilton, Jan Eric Lenssen, Gaurav Rattan, and Martin Grohe. Weisfeiler and leman go neural: Higher-order graph neural networks. In *AAAI Conference on Artificial Intelligence (AAAI)*, pages 4602–4609, 2019.

[39] Luiz Manella Pereira and M. Hadi Amini. A survey on optimal transport for machine learning: Theory and applications. *IEEE Access*, 13:26506–26526, 2025.

[40] Rihong Qiu, Xinke Jiang, Yuchen Fang, Hongbin Lai, Hao Miao, Xu Chu, Junfeng Zhao, and Yasha Wang. Efficient graph continual learning via lightweight graph neural tangent kernels-based dataset distillation. In *International Conference on Machine Learning (ICML)*, 2025.

[41] Si Si, Felix X. Yu, Ankit Singh Rawat, Cho-Jui Hsieh, and Sanjiv Kumar. Serving graph compression for graph neural networks. In *International Conference on Learning Representations (ICLR)*, 2023.

[42] Qingyun Sun, Ziying Chen, Beining Yang, Cheng Ji, Xingcheng Fu, Sheng Zhou, Hao Peng, Jianxin Li, and Philip S. Yu. Gc-bench: An open and unified benchmark for graph condensation. In *Neural Information Processing Systems (NeurIPS)*, 2024.

[43] Titouan Vayer, Laetitia Chapel, Rémi Flamary, Romain Tavenard, and Nicolas Courty.

[44] Petar Velickovic, Guillem Cucurull, Arantxa Casanova, Adriana Romero, Pietro Liò, and Yoshua Bengio. Graph attention networks. In *International Conference on Learning Representations (ICLR)*, 2018.

[45] Cédric Vincent-Cuaz, Rémi Flamary, Marco Corneli, Titouan Vayer, and Nicolas Courty. Semi-relaxed gromov wasserstein divergence with applications on graphs. In *International Conference on Learning Representations (ICLR)*, 2022.

[46] Yuxiang Wang, Xiao Yan, Shiyu Jin, Hao Huang, Quanqing Xu, Qingchen Zhang, Bo Du, and Jiawei Jiang. Self-supervised learning for graph dataset condensation. In *Knowledge Discovery and Data Mining (KDD)*, pages 3289–3298, 2024.

[47] Mingrun Wei, Yeyu Yan, and Dong Wang. Mppq: Enhancing post-training quantization for llms via mixed supervision, proxy rounding, and pre-searching. In *International Joint Conference on Artificial Intelligence IJCAI*, pages 8277–8285, 2025.

[48] Felix Wu, Amauri H. Souza Jr., Tianyi Zhang, Christopher Fifty, Tao Yu, and Kilian Q. Weinberger. Simplifying graph convolutional networks. In *International Conference on Machine Learning (ICML)*, volume 97, pages 6861–6871, 2019.

[49] Zhenbang Xiao, Yu Wang, Shunyu Liu, Huiqiong Wang, Mingli Song, and Tongya Zheng. Simple graph condensation. In *Machine Learning and Knowledge Discovery in Databases (ECML PKDD)*, volume 14942, pages 53–71, 2024.

[50] Zhe Xu, Yuzhong Chen, Menghai Pan, Huiyuan Chen, Mahashweta Das, Hao Yang, and Hanghang Tong. Kernel ridge regression-based graph dataset distillation. In *Knowledge Discovery and Data Mining (KDD)*, pages 2850–2861, 2023.

[51] Bo Yan. Federated graph condensation with information bottleneck principles. *arXiv preprint arXiv: 2405.03911*, 2024.

[52] Yeyu Yan, Chao Li, Yanwei Yu, Xiangju Li, and Zhongying Zhao. OSGNN: original graph and subgraph aggregated graph neural network. *Expert Syst. Appl.*, 225:120115, 2023.

[53] Yeyu Yan, Zhongying Zhao, Zhan Yang, Yanwei Yu, and Chao Li. A fast and robust attention-free heterogeneous graph convolutional network. *IEEE Trans. Big Data*, 10(5):669–681, 2024.

[54] Beining Yang, Qingyun Sun, Cheng Ji, Xingcheng Fu, and Jianxin Li. St-gcond: Self-supervised and transferable graph dataset condensation. In *International Conference on Learning Representations (ICLR)*, 2025.

[55] Beining Yang, Kai Wang, Qingyun Sun, Cheng Ji, Xingcheng Fu, Hao Tang, Yang You, and Jianxin Li. Does graph distillation see like vision dataset counterpart? In *Neural Information Processing Systems (NeurIPS)*, 2023.

[56] Shuo Yin and Guoqiang Zhong. Textgt: A double-view graph transformer on text for aspect-based sentiment analysis. In *AAAI Conference on Artificial Intelligence (AAAI)*, pages 19404–19412, 2024.

[57] Hao Zhang, Xunkai Li, Yinlin Zhu, and Lianglin Hu. Rethinking federated graph learning: A data condensation perspective. *arXiv preprint arXiv:2505.02573*, 2025.

[58] Wentao Zhang, Ziqi Yin, Zeang Sheng, Yang Li, Wen Ouyang, Xiaosen Li, Yangyu Tao, Zhi Yang, and Bin Cui. Graph attention multi-layer perceptron. In *Knowledge Discovery and Data Mining (KDD)*, pages 4560–4570, 2022.

[59] Yuchen Zhang, Tianle Zhang, Kai Wang, Ziyao Guo, Yuxuan Liang, Xavier Bresson, Wei Jin, and Yang You. Navigating complexity: Toward lossless graph condensation via expanding window matching. In *International Conference on Machine Learning (ICML)*, 2024.

[60] Zhongjian Zhang, Xiao Wang, Huichi Zhou, Yue Yu, Mengmei Zhang, Cheng Yang, and Chuan Shi. Can large language models improve the adversarial robustness of graph neural networks? In *Knowledge Discovery and Data Mining (KDD)*, pages 2008–2019, 2025.

[61] Bo Zhao, Konda Reddy Mopuri, and Hakan Bilen. Dataset condensation with gradient matching. In *International Conference on Learning Representations (ICLR)*, 2021.

[62] Ganlong Zhao, Guanbin Li, Yipeng Qin, and Yizhou Yu. Improved distribution matching for dataset condensation. In *Computer Vision and Pattern Recognition (CVPR)*, pages 7856–7865, 2023.

[63] Shuai Zheng, Zhenfeng Zhu, Zhizhe Liu, Youru Li, and Yao Zhao. Node-oriented spectral filtering for graph neural networks. *IEEE Trans. Pattern Anal. Mach. Intell.*, 46(1):388–402, 2024.

[64] Xin Zheng, Miao Zhang, Chunyang Chen, Quoc Viet Hung Nguyen, Xingquan Zhu, and Shirui Pan. Structure-free graph condensation: From large-scale graphs to condensed graph-free data. In *Neural Information Processing Systems (NeurIPS)*, 2023.

[65] Hao Zhu and Piotr Koniusz. Simple spectral graph convolution. In *International Conference on Learning Representations (ICLR)*, 2021.

NeurIPS Paper Checklist

The checklist is designed to encourage best practices for responsible machine learning research, addressing issues of reproducibility, transparency, research ethics, and societal impact. Do not remove the checklist: **The papers not including the checklist will be desk rejected.** The checklist should follow the references and follow the (optional) supplemental material. The checklist does NOT count towards the page limit.

Please read the checklist guidelines carefully for information on how to answer these questions. For each question in the checklist:

- You should answer [Yes] , [No] , or [NA] .
- [NA] means either that the question is Not Applicable for that particular paper or the relevant information is Not Available.
- Please provide a short (1–2 sentence) justification right after your answer (even for NA).

The checklist answers are an integral part of your paper submission. They are visible to the reviewers, area chairs, senior area chairs, and ethics reviewers. You will be asked to also include it (after eventual revisions) with the final version of your paper, and its final version will be published with the paper.

The reviewers of your paper will be asked to use the checklist as one of the factors in their evaluation. While "[Yes] " is generally preferable to "[No] ", it is perfectly acceptable to answer "[No] " provided a proper justification is given (e.g., "error bars are not reported because it would be too computationally expensive" or "we were unable to find the license for the dataset we used"). In general, answering "[No] " or "[NA] " is not grounds for rejection. While the questions are phrased in a binary way, we acknowledge that the true answer is often more nuanced, so please just use your best judgment and write a justification to elaborate. All supporting evidence can appear either in the main paper or the supplemental material, provided in appendix. If you answer [Yes] to a question, in the justification please point to the section(s) where related material for the question can be found.

IMPORTANT, please:

- **Delete this instruction block, but keep the section heading "NeurIPS paper checklist"**,
- **Keep the checklist subsection headings, questions/answers and guidelines below.**
- **Do not modify the questions and only use the provided macros for your answers**.

1. **Claims**

   Question: Do the main claims made in the abstract and introduction accurately reflect the paper's contributions and scope?

   Answer: [Yes]

   Justification: The contributions are empirically validated in the main body.

   Guidelines:

   - The answer NA means that the abstract and introduction do not include the claims made in the paper.
   - The abstract and/or introduction should clearly state the claims made, including the contributions made in the paper and important assumptions and limitations. A No or NA answer to this question will not be perceived well by the reviewers.
   - The claims made should match theoretical and experimental results, and reflect how much the results can be expected to generalize to other settings.
   - It is fine to include aspirational goals as motivation as long as it is clear that these goals are not attained by the paper.

2. **Limitations**

   Question: Does the paper discuss the limitations of the work performed by the authors?

   Answer: [Yes]

   Justification: We discuss the limitations in Appendix E.2.

Guidelines:

- The answer NA means that the paper has no limitation while the answer No means that the paper has limitations, but those are not discussed in the paper.
- The authors are encouraged to create a separate "Limitations" section in their paper.
- The paper should point out any strong assumptions and how robust the results are to violations of these assumptions (e.g., independence assumptions, noiseless settings, model well-specification, asymptotic approximations only holding locally). The authors should reflect on how these assumptions might be violated in practice and what the implications would be.
- The authors should reflect on the scope of the claims made, e.g., if the approach was only tested on a few datasets or with a few runs. In general, empirical results often depend on implicit assumptions, which should be articulated.
- The authors should reflect on the factors that influence the performance of the approach. For example, a facial recognition algorithm may perform poorly when image resolution is low or images are taken in low lighting. Or a speech-to-text system might not be used reliably to provide closed captions for online lectures because it fails to handle technical jargon.
- The authors should discuss the computational efficiency of the proposed algorithms and how they scale with dataset size.
- If applicable, the authors should discuss possible limitations of their approach to address problems of privacy and fairness.
- While the authors might fear that complete honesty about limitations might be used by reviewers as grounds for rejection, a worse outcome might be that reviewers discover limitations that aren't acknowledged in the paper. The authors should use their best judgment and recognize that individual actions in favor of transparency play an important role in developing norms that preserve the integrity of the community. Reviewers will be specifically instructed to not penalize honesty concerning limitations.

3. **Theory Assumptions and Proofs**

   Question: For each theoretical result, does the paper provide the full set of assumptions and a complete (and correct) proof?

   Answer: [Yes]

   Justification: The complete proofs are provide in Appendix A.

   Guidelines:

   - The answer NA means that the paper does not include theoretical results.
   - All the theorems, formulas, and proofs in the paper should be numbered and cross-referenced.
   - All assumptions should be clearly stated or referenced in the statement of any theorems.
   - The proofs can either appear in the main paper or the supplemental material, but if they appear in the supplemental material, the authors are encouraged to provide a short proof sketch to provide intuition.
   - Inversely, any informal proof provided in the core of the paper should be complemented by formal proofs provided in appendix or supplemental material.
   - Theorems and Lemmas that the proof relies upon should be properly referenced.

4. **Experimental Result Reproducibility**

   Question: Does the paper fully disclose all the information needed to reproduce the main experimental results of the paper to the extent that it affects the main claims and/or conclusions of the paper (regardless of whether the code and data are provided or not)?

   Answer: [Yes]

   Justification: We provide a detailed description of PreGC and the parameters for imple menting the baseline in Section 5.1 and the Appendix C.3.

   Guidelines:

   - The answer NA means that the paper does not include experiments.

- If the paper includes experiments, a No answer to this question will not be perceived well by the reviewers: Making the paper reproducible is important, regardless of whether the code and data are provided or not.
- If the contribution is a dataset and/or model, the authors should describe the steps taken to make their results reproducible or verifiable.
- Depending on the contribution, reproducibility can be accomplished in various ways. For example, if the contribution is a novel architecture, describing the architecture fully might suffice, or if the contribution is a specific model and empirical evaluation, it may be necessary to either make it possible for others to replicate the model with the same dataset, or provide access to the model. In general. releasing code and data is often one good way to accomplish this, but reproducibility can also be provided via detailed instructions for how to replicate the results, access to a hosted model (e.g., in the case of a large language model), releasing of a model checkpoint, or other means that are appropriate to the research performed.
- While NeurIPS does not require releasing code, the conference does require all submissions to provide some reasonable avenue for reproducibility, which may depend on the nature of the contribution. For example
  (a) If the contribution is primarily a new algorithm, the paper should make it clear how to reproduce that algorithm.
  (b) If the contribution is primarily a new model architecture, the paper should describe the architecture clearly and fully.
  (c) If the contribution is a new model (e.g., a large language model), then there should either be a way to access this model for reproducing the results or a way to reproduce the model (e.g., with an open-source dataset or instructions for how to construct the dataset).
  (d) We recognize that reproducibility may be tricky in some cases, in which case authors are welcome to describe the particular way they provide for reproducibility. In the case of closed-source models, it may be that access to the model is limited in some way (e.g., to registered users), but it should be possible for other researchers to have some path to reproducing or verifying the results.

5. **Open access to data and code**

   Question: Does the paper provide open access to the data and code, with sufficient instructions to faithfully reproduce the main experimental results, as described in supplemental material?

   Answer: [Yes]

   Justification: Our code and condensed graph data regarding the testing phase are included in the supplementary materials. We will release our complete code as soon.

   Guidelines:

   - The answer NA means that paper does not include experiments requiring code.
   - Please see the NeurIPS code and data submission guidelines (`https://nips.cc/public/guides/CodeSubmissionPolicy`) for more details.
   - While we encourage the release of code and data, we understand that this might not be possible, so "No" is an acceptable answer. Papers cannot be rejected simply for not including code, unless this is central to the contribution (e.g., for a new open-source benchmark).
   - The instructions should contain the exact command and environment needed to run to reproduce the results. See the NeurIPS code and data submission guidelines (`https://nips.cc/public/guides/CodeSubmissionPolicy`) for more details.
   - The authors should provide instructions on data access and preparation, including how to access the raw data, preprocessed data, intermediate data, and generated data, etc.
   - The authors should provide scripts to reproduce all experimental results for the new proposed method and baselines. If only a subset of experiments are reproducible, they should state which ones are omitted from the script and why.
   - At submission time, to preserve anonymity, the authors should release anonymized versions (if applicable).

- Providing as much information as possible in supplemental material (appended to the paper) is recommended, but including URLs to data and code is permitted.

6. **Experimental Setting/Details**

   Question: Does the paper specify all the training and test details (e.g., data splits, hyperparameters, how they were chosen, type of optimizer, etc.) necessary to understand the results?

   Answer: [Yes]

   Justification: We provide a detailed description of PreGC and the parameters for imple menting the baseline in Section 5.1 and the Appendix C.3.

   Guidelines:

   - The answer NA means that the paper does not include experiments.
   - The experimental setting should be presented in the core of the paper to a level of detail that is necessary to appreciate the results and make sense of them.
   - The full details can be provided either with the code, in appendix, or as supplemental material.

7. **Experiment Statistical Significance**

   Question: Does the paper report error bars suitably and correctly defined or other appropriate information about the statistical significance of the experiments?

   Answer: [Yes]

   Justification: We report the standard deviation for all test results.

   Guidelines:

   - The answer NA means that the paper does not include experiments.
   - The authors should answer "Yes" if the results are accompanied by error bars, confidence intervals, or statistical significance tests, at least for the experiments that support the main claims of the paper.
   - The factors of variability that the error bars are capturing should be clearly stated (for example, train/test split, initialization, random drawing of some parameter, or overall run with given experimental conditions).
   - The method for calculating the error bars should be explained (closed form formula, call to a library function, bootstrap, etc.)
   - The assumptions made should be given (e.g., Normally distributed errors).
   - It should be clear whether the error bar is the standard deviation or the standard error of the mean.
   - It is OK to report 1-sigma error bars, but one should state it. The authors should preferably report a 2-sigma error bar than state that they have a 96% CI, if the hypothesis of Normality of errors is not verified.
   - For asymmetric distributions, the authors should be careful not to show in tables or figures symmetric error bars that would yield results that are out of range (e.g. negative error rates).
   - If error bars are reported in tables or plots, The authors should explain in the text how they were calculated and reference the corresponding figures or tables in the text.

8. **Experiments Compute Resources**

   Question: For each experiment, does the paper provide sufficient information on the computer resources (type of compute workers, memory, time of execution) needed to reproduce the experiments?

   Answer: [Yes]

   Justification: We describe the computational resources used in the Appendix C.3.

   Guidelines:

   - The answer NA means that the paper does not include experiments.
   - The paper should indicate the type of compute workers CPU or GPU, internal cluster, or cloud provider, including relevant memory and storage.

- The paper should provide the amount of compute required for each of the individual experimental runs as well as estimate the total compute.
- The paper should disclose whether the full research project required more compute than the experiments reported in the paper (e.g., preliminary or failed experiments that didn't make it into the paper).

9. **Code Of Ethics**

   Question: Does the research conducted in the paper conform, in every respect, with the NeurIPS Code of Ethics `https://neurips.cc/public/EthicsGuidelines`?

   Answer: [Yes]

   Justification: We do not violate Code of Ethics.

   Guidelines:

   - The answer NA means that the authors have not reviewed the NeurIPS Code of Ethics.
   - If the authors answer No, they should explain the special circumstances that require a deviation from the Code of Ethics.
   - The authors should make sure to preserve anonymity (e.g., if there is a special consideration due to laws or regulations in their jurisdiction).

10. **Broader Impacts**

    Question: Does the paper discuss both potential positive societal impacts and negative societal impacts of the work performed?

    Answer: [Yes]

    Justification: We discuss the potential impacts about fairness and privacy issues.

    Guidelines:

    - The answer NA means that there is no societal impact of the work performed.
    - If the authors answer NA or No, they should explain why their work has no societal impact or why the paper does not address societal impact.
    - Examples of negative societal impacts include potential malicious or unintended uses (e.g., disinformation, generating fake profiles, surveillance), fairness considerations (e.g., deployment of technologies that could make decisions that unfairly impact specific groups), privacy considerations, and security considerations.
    - The conference expects that many papers will be foundational research and not tied to particular applications, let alone deployments. However, if there is a direct path to any negative applications, the authors should point it out. For example, it is legitimate to point out that an improvement in the quality of generative models could be used to generate deepfakes for disinformation. On the other hand, it is not needed to point out that a generic algorithm for optimizing neural networks could enable people to train models that generate Deepfakes faster.
    - The authors should consider possible harms that could arise when the technology is being used as intended and functioning correctly, harms that could arise when the technology is being used as intended but gives incorrect results, and harms following from (intentional or unintentional) misuse of the technology.
    - If there are negative societal impacts, the authors could also discuss possible mitigation strategies (e.g., gated release of models, providing defenses in addition to attacks, mechanisms for monitoring misuse, mechanisms to monitor how a system learns from feedback over time, improving the efficiency and accessibility of ML).

11. **Safeguards**

    Question: Does the paper describe safeguards that have been put in place for responsible release of data or models that have a high risk for misuse (e.g., pretrained language models, image generators, or scraped datasets)?

    Answer: [NA]

    Justification:

    Guidelines:

    - The answer NA means that the paper poses no such risks.

- Released models that have a high risk for misuse or dual-use should be released with necessary safeguards to allow for controlled use of the model, for example by requiring that users adhere to usage guidelines or restrictions to access the model or implementing safety filters.
- Datasets that have been scraped from the Internet could pose safety risks. The authors should describe how they avoided releasing unsafe images.
- We recognize that providing effective safeguards is challenging, and many papers do not require this, but we encourage authors to take this into account and make a best faith effort.

12. **Licenses for existing assets**

    Question: Are the creators or original owners of assets (e.g., code, data, models), used in the paper, properly credited and are the license and terms of use explicitly mentioned and properly respected?

    Answer: [Yes]

    Justification: We cite all sources used and comply with their licenses.

    Guidelines:

    - The answer NA means that the paper does not use existing assets.
    - The authors should cite the original paper that produced the code package or dataset.
    - The authors should state which version of the asset is used and, if possible, include a URL.
    - The name of the license (e.g., CC-BY 4.0) should be included for each asset.
    - For scraped data from a particular source (e.g., website), the copyright and terms of service of that source should be provided.
    - If assets are released, the license, copyright information, and terms of use in the package should be provided. For popular datasets, `paperswithcode.com/datasets` has curated licenses for some datasets. Their licensing guide can help determine the license of a dataset.
    - For existing datasets that are re-packaged, both the original license and the license of the derived asset (if it has changed) should be provided.
    - If this information is not available online, the authors are encouraged to reach out to the asset's creators.

13. **New Assets**

    Question: Are new assets introduced in the paper well documented and is the documentation provided alongside the assets?

    Answer: [NA]

    Justification: We do not release new assets.

    Guidelines:

    - The answer NA means that the paper does not release new assets.
    - Researchers should communicate the details of the dataset/code/model as part of their submissions via structured templates. This includes details about training, license, limitations, etc.
    - The paper should discuss whether and how consent was obtained from people whose asset is used.
    - At submission time, remember to anonymize your assets (if applicable). You can either create an anonymized URL or include an anonymized zip file.

14. **Crowdsourcing and Research with Human Subjects**

    Question: For crowdsourcing experiments and research with human subjects, does the paper include the full text of instructions given to participants and screenshots, if applicable, as well as details about compensation (if any)?

    Answer: [NA]

    Justification: We do not involve crowdsourcing nor research with human subjects.

Guidelines:

- The answer NA means that the paper does not involve crowdsourcing nor research with human subjects.
- Including this information in the supplemental material is fine, but if the main contribution of the paper involves human subjects, then as much detail as possible should be included in the main paper.
- According to the NeurIPS Code of Ethics, workers involved in data collection, curation, or other labor should be paid at least the minimum wage in the country of the data collector.

15. **Institutional Review Board (IRB) Approvals or Equivalent for Research with Human Subjects**

    Question: Does the paper describe potential risks incurred by study participants, whether such risks were disclosed to the subjects, and whether Institutional Review Board (IRB) approvals (or an equivalent approval/review based on the requirements of your country or institution) were obtained?

    Answer: [NA]

    Justification: We do not involve crowdsourcing nor research with human subjects.

    Guidelines:

    - The answer NA means that the paper does not involve crowdsourcing nor research with human subjects.
    - Depending on the country in which research is conducted, IRB approval (or equivalent) may be required for any human subjects research. If you obtained IRB approval, you should clearly state this in the paper.
    - We recognize that the procedures for this may vary significantly between institutions and locations, and we expect authors to adhere to the NeurIPS Code of Ethics and the guidelines for their institution.
    - For initial submissions, do not include any information that would break anonymity (if applicable), such as the institution conducting the review.

16. **Declaration of LLM usage**

    Question: Does the paper describe the usage of LLMs if it is an important, original, or non-standard component of the core methods in this research? Note that if the LLM is used only for writing, editing, or formatting purposes and does not impact the core methodology, scientific rigorousness, or originality of the research, declaration is not required.

    Answer: [NA]

    Justification: The LLMs is not the core methods in this research.

    Guidelines:

    - The answer NA means that the core method development in this research does not involve LLMs as any important, original, or non-standard components.
    - Please refer to our LLM policy (`https://neurips.cc/Conferences/2025/LLM`) for what should or should not be described.

Appendix

This is the appendix of our work: **"Towards Pre-trained Graph Condensation via Optimal Transport"**. In this appendix, we provide more details of the proposed PreGC in terms of theoretical proofs, dataset statistics, method analysis, experimental settings with some additional results, and related works.

A Proof of Propositions

Proposition 3.1. *Suppose that it has an analytical filter $g(\cdot)$ for a GNN model, the performance approximation error $\mathcal{O}_{\mathcal{W}}$ of condensed graph is jointly bounded by the reconstruction term $\mathcal{O}_{\mathcal{Z}}$ and the fitting term $\mathcal{O}_{\mathcal{Y}}$.*

$$\underbrace{\|\mathbf{W}-\tilde{\mathbf{W}}\|_F}_{\mathcal{O}_{\mathcal{W}}} \leq \|\boldsymbol{\mathcal{M}}_{\mathcal{Z}}(\mathbf{Y})\|_F \cdot \underbrace{\|\boldsymbol{\mathcal{M}}_{\mathcal{Z}}(g(\mathbf{L})\mathbf{X})^{\dagger}-(g(\tilde{\mathbf{L}})\tilde{\mathbf{X}})^{\dagger}\|_F}_{\mathcal{O}_{\mathcal{Z}}} + \underbrace{\|\boldsymbol{\mathcal{M}}_{\mathcal{Z}}(\mathbf{Y})-\tilde{\mathbf{Y}}\|_F}_{\mathcal{O}_{\mathcal{Y}}} \cdot \|(g(\tilde{\mathbf{L}})\tilde{\mathbf{X}})^{\dagger}\|_F \tag{16}$$

where $\boldsymbol{\mathcal{M}}_{\mathcal{Z}}(\cdot)$ is any mapping function that aligns $g(\tilde{\mathbf{L}})\tilde{\mathbf{X}}$ and $g(\mathbf{L})\mathbf{X}$ or $\tilde{\mathbf{Y}}$ and $\mathbf{Y}$. $\mathbf{L}=\mathbf{I}_N-\mathbf{A}$ and $\tilde{\mathbf{L}}=\mathbf{I}_M-\tilde{\mathbf{A}}$ are the Laplacian matrices of $\mathcal{G}$ and $\tilde{\mathcal{G}}$.

Proof. Given a GNN with an analytical filtering function $g(\cdot)$, we have $g(\mathbf{L})\mathbf{X}\mathbf{W}=\mathbf{Y}$ on the original graph $\mathcal{G}$ and $g(\tilde{\mathbf{L}})\tilde{\mathbf{X}}\tilde{\mathbf{W}}=\tilde{\mathbf{Y}}$ on the condensed graph $\tilde{\mathcal{G}}$, respectively. Due to $\boldsymbol{\mathcal{M}}_{\mathcal{Z}}(\cdot)$ can align the first dimensions, we also have $\boldsymbol{\mathcal{M}}_{\mathcal{Z}}(g(\mathbf{L})\mathbf{X})\mathbf{W}=\boldsymbol{\mathcal{M}}_{\mathcal{Z}}(\mathbf{Y})$ for $\mathcal{G}$. Therefore, the expression can be denoted as:

$$\begin{aligned}
&\|\mathbf{W}-\tilde{\mathbf{W}}\|_F \\
&= \|\boldsymbol{\mathcal{M}}_{\mathcal{Z}}(g(\mathbf{L})\mathbf{X})^{\dagger}\boldsymbol{\mathcal{M}}_{\mathcal{Z}}(\mathbf{Y})-(g(\tilde{\mathbf{L}})\tilde{\mathbf{X}})^{\dagger}\tilde{\mathbf{Y}}\|_F \\
&= \|\boldsymbol{\mathcal{M}}_{\mathcal{Z}}(g(\mathbf{L})\mathbf{X})^{\dagger}\boldsymbol{\mathcal{M}}_{\mathcal{Z}}(\mathbf{Y})-(g(\tilde{\mathbf{L}})\tilde{\mathbf{X}})^{\dagger}\boldsymbol{\mathcal{M}}_{\mathcal{Z}}(\mathbf{Y})+(g(\tilde{\mathbf{L}})\tilde{\mathbf{X}})^{\dagger}\boldsymbol{\mathcal{M}}_{\mathcal{Z}}(\mathbf{Y})-(g(\tilde{\mathbf{L}})\tilde{\mathbf{X}})^{\dagger}\tilde{\mathbf{Y}}\|_F \\
&\leq \|(\boldsymbol{\mathcal{M}}_{\mathcal{Z}}(g(\mathbf{L})\mathbf{X})^{\dagger}-(g(\tilde{\mathbf{L}})\tilde{\mathbf{X}})^{\dagger})\boldsymbol{\mathcal{M}}_{\mathcal{Z}}(\mathbf{Y})\|_F+\|(g(\tilde{\mathbf{L}})\tilde{\mathbf{X}})^{\dagger}(\boldsymbol{\mathcal{M}}_{\mathcal{Z}}(\mathbf{Y})-\tilde{\mathbf{Y}})\|_F \\
&\leq \|\boldsymbol{\mathcal{M}}_{\mathcal{Z}}(\mathbf{Y})\|_F \cdot \|\boldsymbol{\mathcal{M}}_{\mathcal{Z}}(g(\mathbf{L})\mathbf{X})^{\dagger}-(g(\tilde{\mathbf{L}})\tilde{\mathbf{X}})^{\dagger}\|_F+\|\boldsymbol{\mathcal{M}}_{\mathcal{Z}}(\mathbf{Y})-\tilde{\mathbf{Y}}\|_F \cdot \|(g(\tilde{\mathbf{L}})\tilde{\mathbf{X}})^{\dagger}\|_F
\end{aligned} \tag{17}$$

For the trajectory matching methods [64, 59], they integrated the above objectives into the process of graph condensation, that is:

$$\begin{aligned}
&\arg\min_{\tilde{\mathcal{G}}}\|\mathbf{W}-\tilde{\mathbf{W}}\|_F \Rightarrow \\
&\arg\min_{\tilde{\mathcal{G}}}\Big\{\|\boldsymbol{\mathcal{M}}_{\mathcal{Z}}(\mathbf{Y})\|_F \cdot \underbrace{\|\boldsymbol{\mathcal{M}}_{\mathcal{Z}}(g(\mathbf{L})\mathbf{X})^{\dagger}-(g(\tilde{\mathbf{L}})\tilde{\mathbf{X}})^{\dagger}\|_F}_{\mathcal{O}_{\mathcal{Z}}}+\underbrace{\|\boldsymbol{\mathcal{M}}_{\mathcal{Z}}(\mathbf{Y})-\tilde{\mathbf{Y}}\|_F}_{\mathcal{O}_{\mathcal{Y}}} \cdot \|(g(\tilde{\mathbf{L}})\tilde{\mathbf{X}})^{\dagger}\|_F\Big\}
\end{aligned} \tag{18}$$

According to [16], different matching strategies can be summarized into the same optimization objective. Thus, Proposion 3.1 shows that by minimizing the reconstruction term $\mathcal{O}_{\mathcal{Z}}$ and the fitting term $\mathcal{O}_{\mathcal{Y}}$, the performance derived from $\tilde{\mathcal{G}}$ can be approximated to that of $\mathcal{G}$.

This completes the proof of the proposion. □

Proposition 4.1. *When enough diffusion times $\{\delta t_\tau\}_{\tau=1}^{\mathcal{T}}$ are sampled from the distribution $\mathcal{P}$ over the interval $I=[\delta t_{\min}, 2/\lambda_{\max}(\mathbf{L})]$, the spectral response function is satisfied by sampling coverage over the entire spectral range:*

$$\lim_{\mathcal{T}\to\infty}\Pr(\max_i \sup_{\delta t\in I}\min_{\tau}|\Phi_i(\delta t)-\Phi_i(\delta t_\tau)|<\varphi)=1,\ \forall\varphi>0 \tag{19}$$

where $\Phi_i(\delta t)=e^{-K\delta t\lambda_i}$ is the spectral response function for the i-th eigenvalue λ_i.

Proof. Given a graph $\mathcal{G}=(\mathbf{A},\mathbf{X})$, the diffusion state with diffusion intervals δt_τ at time $T=K\delta t_\tau$ can be denoted as:

$$\mathbf{Z}_T^{\tau}=e^{-K\delta t_\tau\mathbf{L}}\mathbf{X}=\mathbf{U}e^{-K\delta t_\tau\boldsymbol{\Lambda}}\mathbf{U}^{\top}\mathbf{X} \tag{20}$$

For the i-th Laplacian eigenvalue λ_i we write the corresponding spectral response $\Phi_i(\delta t)=e^{-K\lambda_i\delta t}$ with $i=1,\ldots,N$. Here, we begin with the following the lemma to better support Proposition 4.1:

Lemma 1. *For any two different diffusion intervals $\delta t_1, \delta t_2 \in I$, the difference in spectral response is satisfied:*

$$|\Phi_i(\delta t_1) - \Phi_i(\delta t_2)| = K\lambda_i e^{-K\psi_i\lambda_i} |\delta t_1 - \delta t_2| \tag{21}$$

where ψ_i lies between δt_1 and δt_2.

Proof. According to the mean value theorem, for the function $\Phi_i(\delta t_\tau) = e^{-K\delta t_\tau \lambda_i}$, there exist $\psi_i \in [\min(\delta t_1, \delta t_2), \max(\delta t_1, \delta t_2)]$ such that:

$$\begin{aligned} \Phi_i(\delta t_2) - \Phi_i(\delta t_1) &= \Phi_i'(\psi_i)(\delta t_2 - \delta t_1) \\ \Phi_i'(\psi_i) &= -K\lambda_i e^{-K\psi_i\lambda_i} \end{aligned} \tag{22}$$

Taking absolute values on both sides of the equation:

$$|\Phi_i(\delta t_1) - \Phi_i(\delta t_2)| = |e^{-K\delta t_1\lambda_i} - e^{-K\delta t_2\lambda_i}| = K\lambda_i e^{-K\psi_i\lambda_i} \cdot |\delta t_1 - \delta t_2| \tag{23}$$

This completes the proof of the lemma. □

From Lemma 1, each Φ_i is Lipschitz on I with constant:

$$L_i = \sup_{\delta t \in I} \left|\Phi_i'(\delta t)\right| = K\lambda_i e^{-K\lambda_i \delta t_{\min}} \tag{24}$$

Let $L = \max_i L_i = K\lambda_N e^{-K\delta t_{\min}\lambda_N}$, where $\lambda_N = \lambda_{\max}(\mathbf{L})$. According to the lemma, for any $\delta t \in I$, if there exists a sampled point δt_τ such that $|\delta t - \delta t_\tau| < \frac{\varphi}{L}$, then for all i, the spectral response functions satisfy:

$$|\Phi_i(\delta t) - \Phi_i(\delta t_\tau)| = K\lambda_i e^{-K\psi_i\lambda_i} \cdot |\delta t - \delta t_\tau| \le L_i \cdot |\delta t - \delta t_\tau| \le L_i \cdot \frac{\varphi}{L} < \varphi \tag{25}$$

To ensure this condition, we divide the interval $I = [\delta t_{\min}, 2/\lambda_{\max}(\mathbf{L})]$ into $m = \lceil \frac{L \cdot |I|}{\varphi} \rceil = \lceil \frac{L(2/\lambda_{\max}(\mathbf{L}) - \delta t_{\min})}{\varphi} \rceil$ sub-intervals, each of length $\frac{|I|}{m} = \frac{2/\lambda_{\max}(\mathbf{L}) - \delta t_{\min}}{m} < \frac{\varphi}{L}$. Assuming the diffusion times $\{\delta t_\tau\}_{\tau=1}^{\mathcal{T}}$ are sampled from a distribution $\mathcal{P}$ with positive density over I, for each subinterval, the probability that at least one sampling point falls into it is:

$$p = 1 - (1 - p_{\min})^{\mathcal{T}} \tag{26}$$

where $p_{\min} > 0$ is the minimum probability of sampling a point in any subinterval. When $\mathcal{T} \to \infty$, we have $p \to 1$. The probability that all m subintervals have at least one sampling point is p^m, and $p^m \to 1$ when $\mathcal{T} \to \infty$.

When all subintervals contain at least one sampling point, for any $\delta t \in I$, there exists a sampling point δt_τ within the same subinterval or in an adjacent subinterval, with $|\delta t - \delta t_\tau| < \frac{\varphi}{L}$. This ensures that:

$$\max_i \sup_{\delta t \in I} \min_\tau |\Phi_i(\delta t) - \Phi_i(\delta t_\tau)| < \varphi \tag{27}$$

Therefore:

$$\lim_{\mathcal{T} \to \infty} \Pr(\max_i \sup_{\delta t \in I} \min_\tau |\Phi_i(\delta t) - \Phi_i(\delta t_\tau)| < \varphi) = 1, \quad \forall \varphi > 0 \tag{28}$$

That is, when $\mathcal{T}$ is sufficiently large, the probability that the sampling points form a φ-net covering I tends to 1, ensuring coverage of the entire function family $\{\Phi_i(\delta t) = e^{-K\delta t\lambda_i} : i = 1, 2, \ldots, N\}$.

This completes the proof of the proposition. □

B Implementation Details of PreGC

B.1 Algorithm

The detailed algorithm of PreGC is shown in Algorithm 1. In detail, the topology generator GEN(Θ) and the condensed features $\tilde{\mathbf{X}}$ are initialized before condensation. To accelerate the synthesis of the condensed graph, the clustering centers of K-means are adopted as the initialization of the condensed features. Here, GEN(Θ) can be any strategy used to generate graph structure, and

we adopt $\text{Sym}(\text{ReLU}(\frac{\Theta+\Theta^\top}{2}))$ with the symmetric normalization function $\text{Sym}(\cdot)$ for convenience. Then, node representations $\tilde{\mathbf{Z}}_T^\tau$ and $\mathbf{Z}_T^\tau$ are generated via the graph diffusion with stochastic states. By calculating the optimal transport of the two graphs in graph space and representation space, one can obtain the transport plans $\pi_{\mathcal{D}}^*$ and $\pi_{\mathcal{Z}}^*$ respectively, and the transport cost $\mathcal{L}_{cost}$. Plan matching loss can be obtained from the difference between metrics $\pi_{\mathcal{D}}^*$ and $\pi_{\mathcal{Z}}^*$. Finally, the PreGC minimizes the loss $\mathcal{L}_{total}$ by iteratively optimizing Θ and $\tilde{\mathbf{X}}$. Our work signifcantly differs from other GC methods, PreGC truly enables pre-training and provides transparent interpretability of the condensation.

Algorithm 1 Pre-trained Graph Condensation (PreGC)

Require: Real graph $\mathcal{G} = (\mathbf{A}, \mathbf{X})$, learning rates η_1 and η_2
Ensure: A small-scale condensed graph $\tilde{\mathcal{G}} = (\tilde{\mathbf{A}}, \tilde{\mathbf{X}})$ with the mapping matrix $\mathbf{M}$.

/* *Condensation Phase* */
Initialize Θ and $\tilde{\mathbf{X}}$.
for $\tau = 0, 1, \cdots, \mathcal{T} - 1$ **do**
  /* *Graph Diffusion Augmentation* */
  Compute $\tilde{\mathbf{A}} = \text{GEN}(\Theta)$; then $\tilde{\mathcal{G}} = (\tilde{\mathbf{A}}, \tilde{\mathbf{X}})$
  Randomly generate diffusion interval δt_τ
  Graph diffusion on $\mathcal{G}$ and $\tilde{\mathcal{G}}$ to genenrate $\mathbf{Z}_T^\tau$ and $\tilde{\mathbf{Z}}_T^\tau$ according to Eq. (6), respectively
  /* *Transport Plan Matching* */
  Calculate graph transport plan $\pi_{\mathcal{D}}^*$ according to Eq. (8)
  Calculate representaion transport plan $\pi_{\mathcal{Z}}^*$ and transport cost $\mathcal{L}_{cost}$ according to Eq. (9)
  Compute plan matching loss $\mathcal{L}_{plan}$ according to Eq. (10)
  /* *Condensed Graph Updating* */
  Compute total loss $\mathcal{L}_{total} = \mathcal{L}_{cost} + \xi\mathcal{L}_{plan}$
  if $\tau\%(\tau_1 + \tau_2) < \tau_1$ **then**
    Update $\Theta \leftarrow \Theta - \eta_1 \nabla_\Theta \mathcal{L}_{total}$
  else
    Update $\tilde{\mathbf{X}} \leftarrow \tilde{\mathbf{X}} - \eta_2 \nabla_{\tilde{\mathbf{X}}} \mathcal{L}_{total}$
  end if
end for
Compute $\mathbf{M}$ according to Eq. (13) and $\tilde{\mathbf{A}} = \text{GEN}(\Theta)$
return $\tilde{\mathbf{A}}$, $\tilde{\mathbf{X}}$, and $\mathbf{M}$

B.2 Details of Optimal Transport Solution

Since Eq. (9) can be regarded as a special form of Eq. (8) (i.e., $\gamma = 1$), our discussion primarily focuses on solving for $\pi_{\mathcal{D}}$ in Eq. (8).

Eq. (8) decomposes into two terms: the former is a Wasserstein distance that operates solely on node features. This term can be efficiently approximated using the Sinkhorn-Knopp algorithm [11], which iteratively converges to the optimal transport plan π^*. Specifically, the Sinkhorn-Knopp algorithm introduces an entropy regularizer and alternates between Sinkhorn projections, $\pi^{(0)} = \exp(-\boldsymbol{\mathcal{K}}(\mathbf{X}, \tilde{\mathbf{X}})/\lambda)$ and $\pi^{(l+1)} = \mathcal{F}_1(\mathcal{F}_2(\pi^{(l)}))$, where l represents the number of iterations and λ denotes the weigth of regularization. The projections $\mathcal{F}_1(\pi) = \pi \oslash (\mathbf{1}\mathbf{1}^\top \pi)$ and $\mathcal{F}_2(\pi) = \pi \oslash (\pi \mathbf{1}\mathbf{1}^\top)$ denote the column normalization and row normalization, respectively, where $\oslash$ is element-wise division. They ensure that the rows and columns satisfy the given marginal distribution constraints. In the limit, this alternating projection will converge to a minimizer $\lim_{t\to\infty} \pi^{(t)} = \pi^*$.

The latter term corresponds to a Gromov-Wasserstein (GW) distance, which can be formulated as a nonconvex quadratic programming problem. We use semi-relaxed Gromov-Wasserstein divergence [45] and optimize π with the conditional gradient solver. The gradient of π with respect to the GW term is $\nabla_\pi = 2\boldsymbol{\mathcal{J}}(\mathbf{A}, \tilde{\mathbf{A}}) \otimes \pi$. The conditional gradient algorithm consists in solving a linearization $\langle \mathbf{P}, \nabla_\pi \rangle$ at each iteration, where $\mathbf{P} \in \mathbb{R}^{N \times M}$ the extreme-point solution that arises from the linearized sub-problem solved. It can be solved by gradient descent with a direction $\mathbf{P}^{(l)}\pi^{(l)}$, followed by a line search for the optimal step.

In the optimization process, we utilize the third-party library functions GeomLoss and Python Optimal Transport (POT) to solve Eq. (8) and Eq. (9), respectively.

C Experimental Details

C.1 Dataset Details

In this work, five graph datasets are adopted to evaluate the effectiveness of our condensation method. and their data statistics are shown in Table D1. Among them, three citation networks (Cora, Citeseer, and Pubmed) [26] are used for node classification (NC), graph clustering (GC), and link prediction (LP) tasks. OGB-Arxiv [60] is used to test the performance of GNNs on topic classification and publication year prediction tasks. H&M [2] is a subset that is obtained from a co-purchase network of products from the H&M company. The nodes are products whose features consist of the product's graphical appearance, perceived color, etc., and they are connected to edges if they are frequently purchased by the same user. H&M has two semi-supervised tasks: predict the categories of products (node classification) and predict their average prices (node regression).

Table D1: Details of dataset statistics. NC, NClu, LP, and NR denotes node classification, node clustering, link prediction, and node regression tasks respectively.

Dataset	Nodes	Edges	Features	Task	Classes	Traing / Validation / Test
Cora	2,708	5,429	1,433	NC / NClu / LP	7	140 / 500 / 1,000
Citeseer	3,327	4,732	3,703	NC / NClu / LP	6	120 / 500 / 1,000
Pubmed	19,717	44,338	500	NC / NClu / LP	3	60 / 500 / 1,000
OGB-Arxiv	14,167	33,520	128	NC-Topic (T)	40	4,585 / 2,517 / 7,065
				NC-Year (Y)	5	7,125 / 3,492 / 3,550
H&M	15,508	920,284	191	NC-Category (C)	21	7,837 / 3,908 / 3,763
				NR-Price (P)	-	7,724 / 3,843 / 3,941

C.2 Baselines & GNNs

Baselines. In this work, six baselines have been selected for comparison.

- **GCDM** [32]: An efficient GC method that generates condensed graphs based on distribution matching by optimizing the maximum mean discrepancy between class representations.
- **GCond** [25]: A representation GC method that utilizes the gradient matching to align the model gradient from both graphs.
- **SFGC** [64]: The first structure-free GC method that synthesizes condensed features by trajectory matching while preserving the topological information of the original graph.
- **SGDD** [55]: A generalized graph condensation method with enhanced graph structure modeling by topological mapping.
- **GDEM** [33]: A GC method for topology enhancement by eigenbasis matching.
- **CGC** [16]: An efficient GC method with graph generation that introduces the training-free strategy in distribution matching.

To illustrate the distinctions among various approaches and emphasize our contributions, we present the relationship between six representative graph condensation methods and the generalized graph condensation paradigm, as shown in Table D2.

GNN architectures. To evaluate and compare the generalization of PreGC and other graph condensation methods, we test the node classification performance with nine different GNN architectures: SGC [48], GCN [26], APPNP [27], k-GNN [38], GAT [44], GraphSAGE (SAGE) [19], SSGC [65], BernNet (Bern.) [23], and GPRGNN (GPR.) [8]. Note that the focus of our work is on verifying the generalization of condensed graphs rather than the effectiveness of a certain GNN architecture. Therefore, we harmonize the GNN parameters for all datasets to ensure the fairness of the experiments. Concretely, the smoothing factor in APPNP, SSG, and GPR. is uniformly set to 0.1, the numer of attention heads in GAT is set to 4. For GNNs [27, 65, 23, 8] that can capture long-range dependencies, we set the number of propagation layers $K = 5$ by default and $K = 2$ otherwise. For other hyperparameters, we use the combination of parameters provided by PyG by default.

Table D2: Comparison of different graph condensation methods. For convenience, SGC $\tilde{\mathbf{A}}^K\tilde{\mathbf{X}}$ is uniformly set to GNN encoder in condensation, and $\tilde{\mathbf{A}}^{(\delta t)} = (1-\delta t)\mathbf{I} + \delta t\tilde{\mathbf{A}}$.

	Condensation Phase				Testing Phase	
	Label Alignment	Graph Condensation	Optimization Objective	Representaion $\tilde{\mathbf{Z}}$	Graph Interpretability	Task Adaptation
GCDM (Arxiv22)	Before	Distribution Matching	$\mathcal{O}_{\mathcal{Z}}$	$\tilde{\mathbf{A}}\tilde{\mathbf{X}}\|\tilde{\mathbf{A}}^2\tilde{\mathbf{X}}\|\cdots\|\tilde{\mathbf{A}}^K\tilde{\mathbf{X}}$	N/A	Classification
GCond (ICLR22)	Before	Gradient Matching	$\mathcal{O}_{\mathcal{W}}$ (w/o $\mathcal{O}_{\mathcal{Y}}$)	$\tilde{\mathbf{A}}^K\tilde{\mathbf{X}}$	N/A	Classification
SFGC (NeurIPS23)	Before	Trajectory Matching	$\mathcal{O}_{\mathcal{W}}$ (w/o $\mathcal{O}_{\mathcal{Y}}$)	$\mathbf{I}^K\tilde{\mathbf{X}}$	N/A	Classification
SGDD (NeurIPS23)	Before	Gradient Matching	$\mathcal{O}_{\mathcal{W}}$ (w/o $\mathcal{O}_{\mathcal{Y}}$)	$\tilde{\mathbf{A}}^K\tilde{\mathbf{X}}$	Topology	Classification
GDEM (ICML24)	Before	Eigenbasis Matching	$\mathcal{O}_{\mathcal{Z}}$	$\tilde{\mathbf{X}}^\top\tilde{\mathbf{L}}\tilde{\mathbf{X}}$	Topology	Classification
CGC (WWW25)	Before	Distribution Matching	$\mathcal{O}_{\mathcal{Z}}$	$\tilde{\mathbf{A}}^K\tilde{\mathbf{X}}$	N/A	Classification
PreGC (Our)	After	Transport Plan Matching	$\mathcal{O}_{\mathcal{Z}}, \mathcal{O}_{\mathcal{Y}}$	$[\tilde{\mathbf{A}}^{(\delta t)}]^K\tilde{\mathbf{X}}$	Semantics	Any Tasks

C.3 Experimental Setup

Task setting. Unless otherwise noted, we use the default training/validation/testing ratios to evaluate the performance of the condensed graphs for supervised tasks. Specifically, for Whole , the training set of the original graph is used for training. For graph condensation methods, we train on the condensed graph, and validation and testing are always evaluated on the validation and test sets of the original graph. For link prediction task, we follow [42] and randomly select 10% ratio of edges as validation and test sets, respectively. In node clustering task, the K-means algorithm is adopted to the learned embeddings of all nodes (For example, "NC→NClu" is denoted as the embedding obtained after training on node classification as input for clustering) and adopts normalized mutual information (NMI) to assess the quality of the clustering results. We report test accuracy (%) on NC, NMI (%) on NClu, AUC (%) on LP and R^2 (%) on NR tasks. The average results and standard deviations of performing 5 different random seeds on each task are reported.

Condensation setting. For condensation methods, the hyperparameters are set according to the original paper if available. Otherwise, we follow the hyperparameter combinations in GC-Bench [42]. Except for the OGB-Arxiv dataset which uses the normalized features provided by [60], all other graph data are condensed using the original features. For our proposed PreGC, we set the importance coefficient $\gamma = 0.5$ in Eq. (8) by default, $\delta t_{\text{min}} = 0.1$ for all datasets.

Evaluation setting. To verify the effectiveness of various graph condensation strategies, all graphs, except H&M adopt one-layer GNN encoder, are uniformly configured with a two-layer SGC as the GNN encoder and a single-layer MLP as the predictor by default to adapt to different downstream tasks. For all GNNs, the hidden unit is set to 64, with a learning rate of 0.01, weight decay of 0.0005 and the Adam optimizer employed.

Experiment environment. The experiments are conducted on the machine with Intel(R) Xeon(R) Silver 4314 CPU @ 2.40GHz, and NVIDIA GeForce RTX 4090 with 24GB memory and CUDA 12.0. The operating system is Ubuntu 20.04.6 with 384GB memory.

D More Experimental Results

D.1 Performance of PreGC on OGB-Arxiv and H&M datasets.

In this section, we show the experimental results at other condensation ratios, as shown in Table E1. For transfer tasks such as "Y→T", the condensed graph is first generated on the source task "Y". The testing phase involves: (1) computing the transport plan between original and condensed graphs, then (2) transferring the labels of task "T" from the original graph to the condensed graph for evaluation.

In particular, existing condensation methods are incompatible with node regression tasks, making condensed graphs unavailable when the source task is "P". Not surprisingly, PreGC consistently outperforms existing GC methods. In particular, the fine-tuning PreGC,i.e., PreGC$_{\text{ft}}$, achieves more significant gains on the transfer task. This suggests that the semantic distribution will be significantly different for different tasks. However, existing methods can only be adapted to a single categorization task, resulting in limited application of their condensed graphs.

Table E1: Performance comparison to baselines on different supervised tasks.

	OGB-Arxiv ($r = 2.5\%$)				H&M ($r = 5.0\%$)			
	T→T	Y→T	Y→Y	T→Y	C→C	P→C	P→P	C→P
Whole	64.43 ± 0.24		55.37 ± 0.21		77.07 ± 0.26		50.80 ± 0.64	
GCDM	35.49±3.01	44.59±1.59	45.69±0.95	34.66±3.24	59.69±1.18	N/A	N/A	19.23±1.87
Gcond	58.49±0.63	49.92±1.66	48.88±1.05	47.18±1.06	51.94±2.71	N/A	N/A	15.35±1.46
SFGC	59.72±0.26	47.93±0.57	50.06±0.56	45.66±1.06	59.31±2.28	N/A	N/A	14.94±0.55
SGDD	60.46±0.33	51.84±0.40	49.89±0.53	44.50±1.64	62.44±0.51	N/A	N/A	17.75±3.19
GDEM	56.69±0.70	34.19±0.03	49.94±0.63	48.54±0.62	51.71±0.89	N/A	N/A	11.73±1.72
CGC	59.71±0.42	56.78±1.23	50.79±0.29	49.71±0.54	66.60±0.29	N/A	N/A	29.79±0.64
PreGC	62.66±0.47	61.99±0.49	52.96±0.35	52.05±0.42	71.06±0.26	69.38±0.41	36.94±1.05	36.23±0.87
Imp.	2.20↑	5.21↑	2.17↑	2.34↑	4.46↑	-	-	6.44↑
PreGC$_{\text{ft}}$	**62.90±0.49**	**62.85±0.48**	**53.11±0.17**	**53.20±0.21**	**71.54±0.40**	**71.44±0.32**	**37.07±0.96**	**37.01±0.94**
Imp.	2.44↑	6.07↑	2.32↑	3.49↑	4.94↑	-	-	7.22↑

D.2 Generalization Ability of PreGC across Different GNNs.

This section presents additional generalization results of PreGC across different GNNs, as detailed in Tables E2-E4. Overall, the condensed graphs synthesized via PreGC consistently outperform other condensation methods across diverse datasets, demonstrating the effectiveness of graph diffusion augmentation. While the most competitive baseline CGC surpasses PreGC on certain GNNs, its performance remains limited to specific architectures and shows inferior results on some spatial GNNs (e.g., k-GNN and GraphSAGE).

Table E2: Node classification performance across different GNNs on Cora ($r = 2.6\%$) (Highlight marks the lossless results and **Avg.** is the average results of GNNs).

	SGC	GCN	APPNP	k-GNN	GAT	SAGE	SSGC	Bern.	GPR.	**Avg.**
Whole	80.8±0.8	81.0±0.6	81.9±0.8	77.7±1.0	81.8±0.8	79.4±0.5	81.3±0.6	81.5±0.3	81.2±0.8	80.7±1.4
GCDM	69.2±0.4	67.4±0.9	74.3±0.3	44.8±2.3	68.2±0.8	46.6±1.1	73.9±0.7	70.4±1.2	66.4±2.5	64.6±11.1
GCond	79.0±0.6	79.1±0.5	78.7±0.8	63.2±3.1	73.3±1.6	66.7±1.5	78.5±1.1	74.4±3.0	72.0±1.6	73.9±5.8
SFGC	79.2±1.4	80.0±0.5	80.3±0.5	78.2±0.7	79.9±0.7	77.5±0.6	80.7±0.7	80.0±0.7	79.6±0.4	79.5±1.0
SGDD	81.1±0.8	79.8±0.7	81.2±1.4	71.3±2.6	79.2±0.6	77.4±0.9	80.2±1.0	79.5±2.4	78.8±1.4	78.7±3.0
GDEM	80.8±0.4	80.8±0.4	81.1±0.9	78.6±0.7	80.3±0.4	79.1±0.4	81.2±0.3	80.9±0.5	80.6±0.4	80.4±0.9
CGC	**81.8±0.6**	81.5±0.9	81.6±0.8	40.4±7.0	**81.0±0.9**	66.4±1.2	81.1±0.3	**81.7±0.6**	81.4±0.6	75.2±14.0
PreGC	81.6±0.9	**81.84±1.1**	**82.3±0.4**	**78.8±1.0**	80.0±1.0	**79.8±0.6**	**82.1±1.0**	81.1±0.5	**82.3±0.6**	**81.1±1.3**

Table E3: Node classification performance across different GNNs on Citeseer ($r = 0.9\%$).

	SGC	GCN	APPNP	k-GNN	GAT	SAGE	SSGC	Bern.	GPR.	**Avg.**
Whole	69.2±0.4	69.6±0.33	69.9±0.7	65.5±1.3	69.5±0.7	70.0±0.6	69.8±0.7	68.2±1.0	69.4±0.9	69.0±1.4
GCDM	54.7±1.2	55.1±0.9	56.4±1.6	33.7±1.2	56.1±1.2	41.7±1.2	55.9±1.5	51.9±0.7	49.2±1.9	50.5±7.9
GCond	68.9±1.0	70.1±0.7	60.1±1.3	52.0±3.4	49.4±5.9	62.7±1.1	60.7±2.0	59.9±4.0	48.8±5.8	59.2±7.8
SFGC	67.1±0.9	69.4±0.6	65.7±2.4	66.0±2.2	65.4±1.6	65.7±0.7	68.4±0.9	63.2±2.2	69.0±0.8	66.6±2.0
SGDD	68.9±1.6	69.1±1.4	70.6±1.0	69.0±1.9	62.1±4.2	**70.2±0.6**	69.9±1.2	65.3±3.0	64.0±2.9	67.7±3.1
GDEM	70.6±0.3	69.2±0.8	70.1±0.6	68.6±0.7	69.2±0.7	68.4±0.7	69.5±0.3	69.2±0.8	69.5±0.4	69.4±0.7
CGC	70.5±0.4	**72.4±0.5**	**71.5±0.7**	63.3±2.0	70.4±0.8	63.0±1.3	**72.2±0.8**	**72.2±0.5**	64.9±1.0	68.9±4.0
PreGC	**70.6±0.5**	69.3±1.5	69.9±0.7	**69.1±0.5**	**71.0±1.0**	69.1±0.7	69.9±0.4	69.5±0.7	**69.9±1.3**	**69.8±0.7**

D.3 Performance Gap between Condensed Graph and Original Graph

Figs. E1 and E2 show the labeled reconstruction error of different condensation methods. It can be clearly observed that PreGC consistently and significantly outperforms existing graph condensation methods, particularly on the CiteSeer and PubMed datasets. This result not only confirms the effectiveness of PreGC in preserving the critical properties of original graphs during condensation, but also reveals its robustness to architecture dependencies.

Table E4: Node classification performance across different GNNs on OGB-Arxiv-topic ($r = 2.5\%$).

	SGC	GCN	APPNP	k-GNN	GAT	SAGE	SSGC	Bern.	GPR.	**Avg.**
Whole	64.4±0.2	63.8±0.5	65.4±0.5	64.2±0.6	63.8±0.3	61.8±0.2	64.7±0.4	63.0±0.2	64.5±0.8	63.9±1.0
GCDM	35.5±3.0	48.8±1.6	48.9±1.5	36.1±2.0	52.2±1.0	35.3±1.7	48.4±0.7	42.9±3.0	49.6±2.3	44.2±6.9
GCond	58.5±0.6	58.7±0.6	58.1±0.9	27.8±2.6	39.8±4.6	29.2±2.2	60.1±0.2	52.5±1.4	46.8±1.5	47.9±12.9
SFGC	59.7±0.3	58.8±1.1	59.9±0.8	57.0±0.2	59.5±0.5	50.1±1.3	60.4±0.5	57.5±1.9	58.3±0.8	57.9±3.1
SGDD	60.5±0.3	54.7±0.9	56.5±0.9	44.1±2.8	31.1±2.0	41.3±1.9	60.3±0.4	33.9±3.8	37.9±3.1	46.7±11.5
GDEM	56.7±0.7	54.7±1.5	55.3±1.3	35.9±3.9	52.2±0.8	35.0±2.1	55.2±1.0	48.4±2.4	47.0±3.2	48.9±8.3
CGC	59.7±0.4	58.7±0.5	61.8±0.8	31.7±1.1	60.5±0.6	37.6±1.9	60.1±0.2	57.1±1.0	53.9±0.8	53.5±11.0
PreGC	**62.9±0.5**	**62.5±0.7**	**64.9±0.3**	**62.9±0.9**	**61.4±0.6**	**59.5±0.5**	**64.2±0.7**	**59.8±1.5**	**63.2±0.5**	**62.4±1.8**

Table E5: Node classification performance across different GNNs on OGB-Arxiv-year ($r = 2.5\%$).

	SGC	GCN	APPNP	k-GNN	GAT	SAGE	SSGC	Bern.	GPR.	**Avg.**
Whole	55.4±0.2	57.7±0.4	55.9±0.4	56.8±0.5	56.1±0.5	54.5±0.6	55.6±0.4	53.9±0.6	54.2±0.3	55.5±1.3
GCDM	45.7±1.0	50.0±0.1	48.1±0.8	51.0±0.2	50.9±0.2	43.7±1.1	50.2±0.4	41.8±2.1	49.9±0.7	47.9±3.4
GCond	48.9±1.1	50.8±0.2	50.8±0.5	31.2±4.6	50.9±0.4	41.9±0.9	51.2±0.2	49.6±0.4	50.2±0.3	47.3±6.7
SFGC	50.1±0.6	52.0±0.5	51.3±0.3	51.4±0.4	51.9±0.5	45.4±1.2	51.4±0.4	**51.3±0.1**	51.6±0.1	50.7±2.1
SGDD	49.9±0.5	50.9±0.2	50.7±0.1	51.1±0.0	51.1±0.0	42.4±0.1	50.6±0.4	43.0±3.7	48.5±1.3	48.7±3.5
GDEM	49.9±0.6	51.2±0.3	48.8±0.5	50.9±0.2	51.1±0.3	42.0±1.3	51.2±0.2	43.0±3.1	50.9±0.3	48.8±3.7
CGC	50.8±0.3	51.3±0.1	51.0±0.5	49.1±1.1	51.1±0.4	39.1±0.8	51.2±0.2	50.9±0.3	50.9±0.1	49.5±4.0
PreGC	**53.0±0.4**	**53.3±0.3**	**53.5±0.1**	**52.7±0.3**	**53.0±0.2**	**52.1±0.4**	**53.5±0.4**	51.1±1.0	**51.9±0.1**	**52.7±0.8**

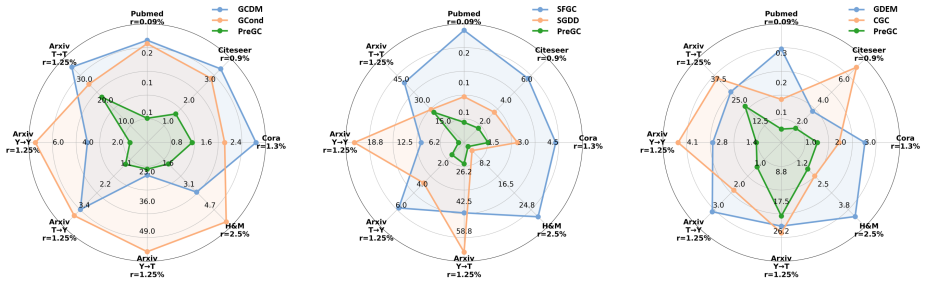

Figure E1: The LRE of different GC methods with the smaller condensation ratio.

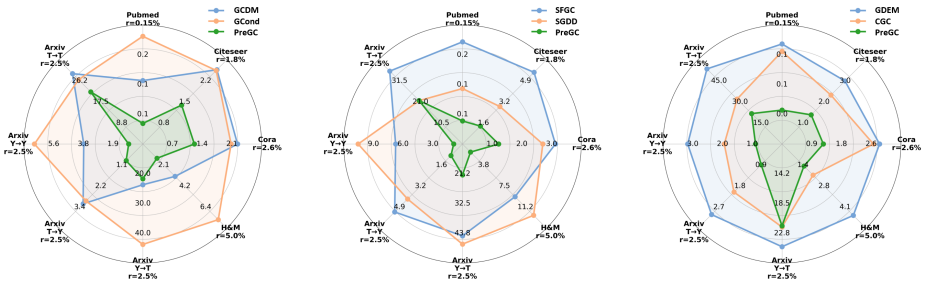

Figure E2: The LRE of different GC methods with the larger condensation ratio.

D.4 Data Valuation based on Node Significance

This section evaluates the node significance of the original graph, i.e., the ability to explicitly represent the importance of the source node through the transport plan. We rescreened the same number of nodes as the original training set based on Eq. (11). For example, in the Cora dataset, the default number of training nodes is 140 (Default), and we select the top-140 raw nodes based on node significance $\mathbf{s}$ and label them as the training nodes. The training nodes selected through the transport plan prove more valuable than the default training set, yielding significant improvements in the performance of GNN, as shown in Figs. E3 and E4. This matching method not only enhances the effectiveness of data annotation, but also elucidates the relative influence of different nodes during the condensation process, thereby improving the interpretability of graph condensation.

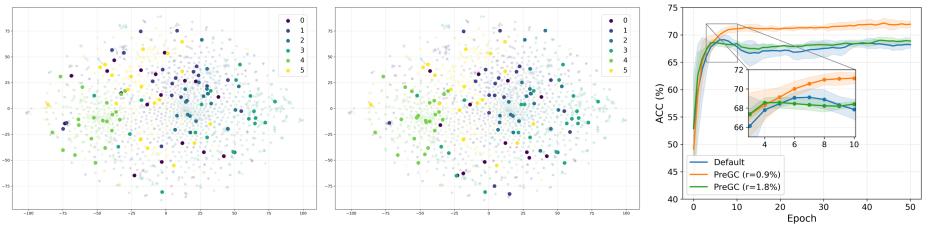

(a) Default ($\bar{d} = 2.88$) (b) PreGC-0.9% ($\bar{d} = 3.03$) (c) Performance on Citeseer

Figure E3: Performance of training set selected with transport plan on Citeseer.

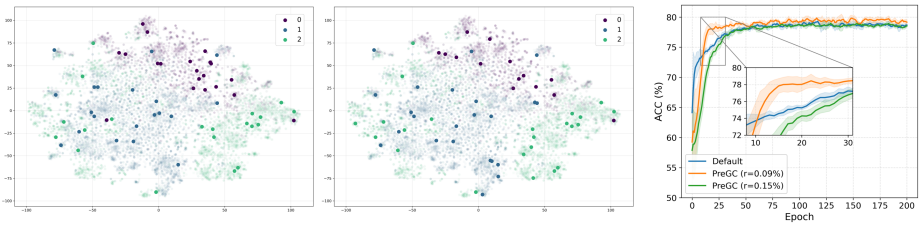

(a) Default ($\bar{d} = 0.172$) (b) PreGC-0.09% ($\bar{d} = 0.174$) (c) Performance on Pubmed

Figure E4: Performance of training set selected with transport plan on Pubmed.

D.5 Sensitivity Analysis

Our investigation further examines the sensitivity of several crucial hyperparameters: the loss balancing coefficient ξ in condensation, the iteration interval τ_{up} and the decay rate ϵ in supervised fine-tuning, as illustrated in Fig. E5. The sensitivity to the balance coefficient varies across different datasets. Generally, the best results are achieved when $\xi = 1$ or 2. Fig. E5 (b) illustrates the impact of supervised fine-tuning on the H&M dataset (The dark blue part represents the condensed graph without supervised fine-tuning), where a trade-off between the values of τ_{up} and ϵ is required to ensure optimal performance of PreGC.

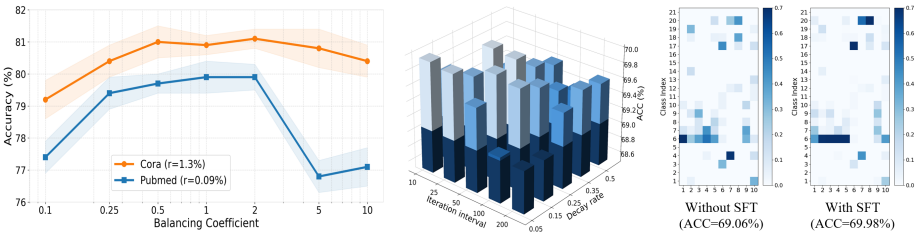

(a) Performance of PreGC with different ξ (b) Performance of PreGC$_{\text{sft}}$ with different τ_{up} and ϵ (c) Label distribution on H&M-category

Figure E5: The impact of different parameter combinations on PreGC.

D.6 Ablation Study

In this section, we add ablation experiments of PreGC on the OGB-Arxiv dataset, with the results presented in Table E6. Consistent with the observations on the H&M dataset, both key modules play a significant role in graph condensation. Notably, the removal of graph diffusion augmentation leads to increased performance fluctuations, which demonstrates that graph diffusion augmentation can enhance the generalization capability of the condensed graph.

Table E6: Experimental results for the ablation study on OGB-Arxiv.

OGB-Arxiv	r=1.25%		r=2.5%	
	Topic	Year	Topic	Year
PreGC	60.55±0.43	52.34±0.30	62.66±0.47	52.96±0.35
PreGC$_{\text{w/o } Aug}$	59.21±0.75	51.10±0.64	59.93±0.68	51.06±0.79
PreGC$_{\text{w/o } \mathcal{L}_{cost}}$	58.84±0.51	49.42±0.58	59.99±0.42	50.55±0.49

D.7 Computational Cost

In this section, we conduct additional experiments to compare the computational efficiency of PreGC with existing baselines on the Cora dataset. It covers peak memory usage and runtime across the pre-processing, condensation, and fine-tuning stages (CGC is excluded as it is a training-free method). The results are shown in Table E7 (* denotes the result of a single execution. Note that in practical implementations, multiple preprocessing often be necessary depending on specific settings.). It can be observed that PreGC achieves significantly faster condensation time compared to most GC methods. Even when fine-tuning is required, it only increases a few additional time costs. Although GDEM spends the least time during the condensation process, it requires extra preprocessing time for eigenvalue decomposition. Overall, both PreGC and GDEM exhibit substantially lower training times than other GC methods. The underlying reason is that existing GC methods employ a nested bi-level optimization: an outer loop updates the GNN parameters, while an inner loop optimizes the condensed graph. In contrast, PreGC leverages graph diffusion, a parameter-free message passing mechanism, eliminating the time-consuming outer loop. This not only reduces condensation time but also prevents the condensed graph from overfitting to architecture-specific parameters. Furthermore, when downstream tasks or label distributions change, existing baselines must re-condense the graph to capture this updated knowledge. In contrast, PreGC is task- and label-agnostic, thus requiring only a single condensation and can be reused multiple times.

Table E7: The computational cost on Cora dataset ($r = 1.3\%$).

	Memory (MB)	**Pre-processing (S)**	**Condensation (S)**	**Fine-tuning (S)**	**Total (S)**
GCDM	1,276	-	1542.38	-	1542.38
GCond	1,280	-	2,304.41	-	2,304.41
SFGC	2,514	14.01*	1,923.64	-	1,937.65
SGDD	1,644	-	2,364.18	-	2,364.18
GDEM	2,658	4.56*	7.48	-	12.04
PreGC	1,714	-	22.36	0.81	23.17

E Discussion

E.1 Related Work

Graph Reduction. Unlike model quantization [47] and knowledge distillation [37], graph reduction [64, 22] is a data-centric approach. It aims to reduce the size of a graph by decreasing the number of nodes and edges, allowing efficient and effective GNN training. It includes graph sparsification [1, 7], graph coarsening [41, 28], and graph condensation [25, 55]. Graph sparsification aims to reduce edge density while preserving key structural or spectral properties of the original graph. Graph coarsening aggregates nodes or edges to form a smaller super-node or super-edge, often maintaining hierarchical relationships. Their core principle is to maintain specific large-scale graph properties (e.g., spectra and principal eigenvalues) in smaller graphs that have been thinned or coarsened, essentially still

modifying the original graph. In contrast, graph condensation directly optimizes and synthesizes a small-scale condensed graph, which breaks the information constraints imposed by the original graph and promotes consistent GNN test performance.

Graph Condensation [25, 24], a.k.a., graph distillation [33], aims to condense large-scale graph data into a small-scale synthetic graph, reducing garph redundancy and accelerating GNN training. Due to its superior ability in graph reduction, it has found a wide range of applications, including accelerating inference [14], graph continuous learning [34], and federated graph learning [51].

Early GC methods inspired by data condensation [61, 62] proposed matching strategies such as gradient matching [25, 24, 13], trajectory matching [64, 59], distribution matching [32, 16, 49], etc., focusing more on learning the consistency of the representation space and proposing a related variant of structure-free. SGDD [55] was the first to propose Laplacian energy distributions to metricize the relationships among structures. GDEM [33] analyzed the upper limit of the existing GC performance is limited by the GNN architecture and improves this problem by eigenbasis matching. In addition, the parameters in different GNNs also bring implicit bias that would be inherited by the condensed graph.[16] and [17] proposed efficient graph condensation without parameters to avoid this problem. [54] synthesized a condensed soft label using multiple self-supervised tasks as auxiliary information to enhance the fitness of condensed graphs. Despite the great efforts made by the above methods, they are still limited to a particular task (e.g., node classification). Recently, SGDC [46] proposed self-supervised graph-level condensation, which is free from task dependency by contrast learning. [15] extended it to self-supervised node-level condensation, improving the generalization ability in condensed graphs on unsupervised tasks. However, the essence of the above methods is still based on class partitioning, which cannot be applied to other supervised tasks (e.g., node regression), hindering the reusability of condensed graphs.

To our best knowledge, we are the first attempt to study generalized graph condensation. PreGC has the advantages of being GNN-parameter-free and task-independent, allowing the condensed graph to be flexibly adapted to arbitrary GNN architectures and diverse downstream tasks.

Applications of Graph Condensation. In addition to the aforementioned research, graph condensation has been further extended to other domains [40, 4]. For example, Jin et al. [24] were the first to generalize graph condensation from node-level to graph-level tasks and significantly reduced condensation cost using one-step gradient matching. Xu et al. [50] reformulated the paradigm of graph-level condensation via kernel ridge regression while preserving the performance of the original graph data. Gupta et al. [18] and Wang et al.[46] further extended graph condensation to model-agnostic and self-supervised graph-level settings, rapidly advancing the field. Moreover, owing to the training efficiency of condensed graphs, Liu et al. [35, 36] integrated graph condensation with continual learning, both mitigating catastrophic forgetting and accelerating model training. Yan et al. [51] and Zhang et al. [57] applied graph condensation to federated graph learning, enabling distributed graph learning under privacy constraints by sharing knowledge through condensed graphs.

E.2 Limitation

Although the proposed PreGC is highly generalizable and reusable, eliminating the need to repeat the condensation, it still suffers from a shortcoming. PreGC inevitably introduces additional complexity to the condensation process due to the computational constraints of optimal transport. Potential improvements in computational efficiency can be explored through graph partitioning techniques or linear optimal transport approximations. However, since the main contribution of this work is to propose a generalized graph condensation paradigm and a pre-trained condensation framework, we defer the study of improving computational efficiency to future research.

E.3 Broader Impacts

Although graph condensation is pivotal for scaling graph neural networks to large-scale graph data, it can also entail fairness and privacy risks. Due to the condensation process selectively preserves or amplifies structural patterns, it may inadvertently over-represent majority groups while suppressing minority substructures. Moreover, the re-synthesis of node features complicates established anonymization guarantees, as condensed features may be re-identified via topological cues. Accordingly, the condensation procedure should be considered to mitigate unfairness induced by structural bias while simultaneously preventing the leakage of sensitive attribute information.